

Trigger and data acquisition

N. Ellis

CERN, Geneva, Switzerland

Abstract

The lectures address some of the issues of triggering and data acquisition in large high-energy physics experiments. Emphasis is placed on hadron-collider experiments that present a particularly challenging environment for event selection and data collection. However, the lectures also explain how T/DAQ systems have evolved over the years to meet new challenges. Some examples are given from early experience with LHC T/DAQ systems during the 2008 single-beam operations.

1 Introduction

These lectures concentrate on experiments at high-energy particle colliders, especially the general-purpose experiments at the Large Hadron Collider (LHC) [1]. These experiments represent a very challenging case that illustrates well the problems that have to be addressed in state-of-the-art high-energy physics (HEP) trigger and data-acquisition (T/DAQ) systems. This is also the area in which the author is working (on the trigger for the ATLAS experiment at LHC) and so is the example that he knows best. However, the lectures start with a more general discussion, building up to some examples from LEP [2] that had complementary challenges to those of the LHC. The LEP examples are a good reference point to see how HEP T/DAQ systems have evolved in the last few years.

Students at this school come from various backgrounds—phenomenology, experimental data analysis in running experiments, and preparing for future experiments (including working on T/DAQ systems in some cases). These lectures try to strike a balance between making the presentation accessible to all, and going into some details for those already familiar with T/DAQ systems.

1.1 Definition and scope of trigger and data acquisition

T/DAQ is the online system that selects particle interactions of potential interest for physics analysis (trigger), and that takes care of collecting the corresponding data from the detectors, putting them into a suitable format and recording them on permanent storage (DAQ). Special modes of operation need to be considered, e.g., the need to calibrate different detectors in parallel outside of normal data-taking periods. T/DAQ is often taken to include associated tasks, e.g., run control, monitoring, clock distribution and book-keeping, all of which are essential for efficient collection and subsequent offline analysis of the data.

1.2 Basic trigger requirements

As introduced above, the trigger is responsible for selecting interactions that are of potential interest for physics analysis. These interactions should be selected with high efficiency, the efficiency should be precisely known (since it enters in the calculation of cross-sections), and there should not be biases that affect the physics results. At the same time, a large reduction of rate from unwanted high-rate processes may be needed to match the capabilities of the DAQ system and the offline computing system. High-rate processes that need to be rejected may be instrumental backgrounds or high-rate physics processes that are not relevant for the analyses that one wants to make. The trigger system must also be affordable, which implies limited computing power. As a consequence, algorithms that need to be executed at high rate must be fast. Note that it is not always easy to achieve the above requirements (high efficiency for signal, strong background rejection and fast algorithms) simultaneously.

Trigger systems typically select events¹ according to a ‘trigger menu’, i.e., a list of selection criteria — an event is selected if one or more of the criteria are met. Different criteria may correspond to different signatures for the same physics process — redundant selections lead to high selection efficiency and allow the efficiency of the trigger to be measured from the data. Different criteria may also reflect the wish to concurrently select events for a wide range of physics studies — HEP ‘experiments’ (especially those with large general-purpose ‘detectors’ or, more precisely, detector systems) are really experimental facilities. Note that the menu has to cover the physics channels to be studied, plus additional data samples required to complete the analysis (e.g., measure backgrounds, and check the detector calibration and alignment).

1.3 Basic data-acquisition requirements

The DAQ system is responsible for the collection of data from detector digitization systems, storing the data pending the trigger decision, and recording data from the selected events in a suitable format. In doing so it must avoid corruption or loss of data, and it must introduce as little dead-time as possible (‘dead-time’ refers to periods when interesting interactions cannot be selected — see below). The DAQ system must, of course, also be affordable which, for example, places limitations on the amount of data that can be read out from the detectors.

2 Design of a trigger and data-acquisition system

In the following a very simple example is used to illustrate some of the main issues for designing a T/DAQ system. An attempt is made to omit all the detail and concentrate only on the essentials — examples from real experiments will be discussed later.

Before proceeding to the issue of T/DAQ system design, the concept of dead-time, which will be an important element in what follows, is introduced. ‘Dead-time’ is generally defined as the fraction or percentage of total time where valid interactions could not be recorded for various reasons. For example, there is typically a minimum period between triggers — after each trigger the experiment is dead for a short time.

Dead-time can arise from a number of sources, with a typical total of up to $\mathcal{O}(10\%)$. Sources include readout and trigger dead-time, which are addressed in detail below, operational dead-time (e.g., time to start/stop data-taking runs), T/DAQ downtime (e.g., following a computer failure), and detector downtime (e.g., following a high-voltage trip). Given the huge investment in the accelerators and the detectors for a modern HEP experiment, it is clearly very important to keep dead-time to a minimum.

In the following, the design issues for a T/DAQ system are illustrated using a very simple example. Consider an experiment that makes a time-of-flight measurement using a scintillation-counter telescope, read out with time-to-digital converters (TDCs), as shown in Fig. 1. Each plane of the telescope is viewed by a photomultiplier tube (PMT) and the resulting electronic signal is passed to a ‘discriminator’ circuit that gives a digital pulse with a sharp leading edge when a charged particle passes through the detector. The leading edge of the pulse appears a fixed time after the particle traverses the counter. (The PMTs and discriminators are not shown in the figure.)

Two of the telescope planes are mounted close together, while the third is located a considerable distance downstream giving a measurable flight time that can be used to determine the particle’s velocity. The trigger is formed by requiring a coincidence (logical AND) of the signals from the first two planes, avoiding triggers due to random noise in the photomultipliers — it is very unlikely for there to be noise pulses simultaneously from both PMTs. The time of arrival of the particle at the three telescope planes is measured, relative to the trigger signal, using three channels of a TDC. The pulses going to the TDC from each of the three planes have to be delayed so that the trigger signal, used to start the TDC (analogous to starting a stop-watch), gets there first.

¹The term ‘event’ will be discussed in Section 3 — for now, it may be taken to mean the record of an interaction.

The trigger signal is also sent to the DAQ computer, telling it to initiate the readout. Not shown in Fig.1 is logic that prevents further triggers until the data from the TDC have been read out into the computer — the so-called dead-time logic.

2.1 Traditional approach to trigger and data acquisition

The following discussion starts by presenting a ‘traditional’ approach to T/DAQ (as might be implemented using, for example, NIM and CAMAC electronics modules², plus a DAQ computer). Note that this approach is still widely used in small test set-ups. The limitations of this model are described and ways of improving on it are presented. Of course, a big HEP experiment has an enormous number of sensor channels [up to $\mathcal{O}(10^8)$ at LHC], compared to just three in the example. However, the principles are the same, as will be shown later.

Limitations of the T/DAQ system shown in Fig. 1 are as follows:

1. The trigger decision has to be made very quickly because the TDCs require a ‘start’ signal that arrives before the signals that are to be digitized (a TDC module is essentially a multichannel digital stop-watch). The situation is similar with traditional analog-to-digital converters (ADCs) that digitize the magnitude of a signal arriving during a ‘gate’ period, e.g., the electric charge in an analog pulse — the gate has to start before the pulse arrives.
2. The readout of the TDCs by the computer may be quite slow, which implies a significant dead-time if the trigger rate is high. This limitation becomes much more important in larger systems, where many channels have to be read out for each event. For example, if 1000 channels have to be read out with a readout time of 1 μs per channel (as in CAMAC), the readout time per event is 1 ms which excludes event rates above 1 kHz.

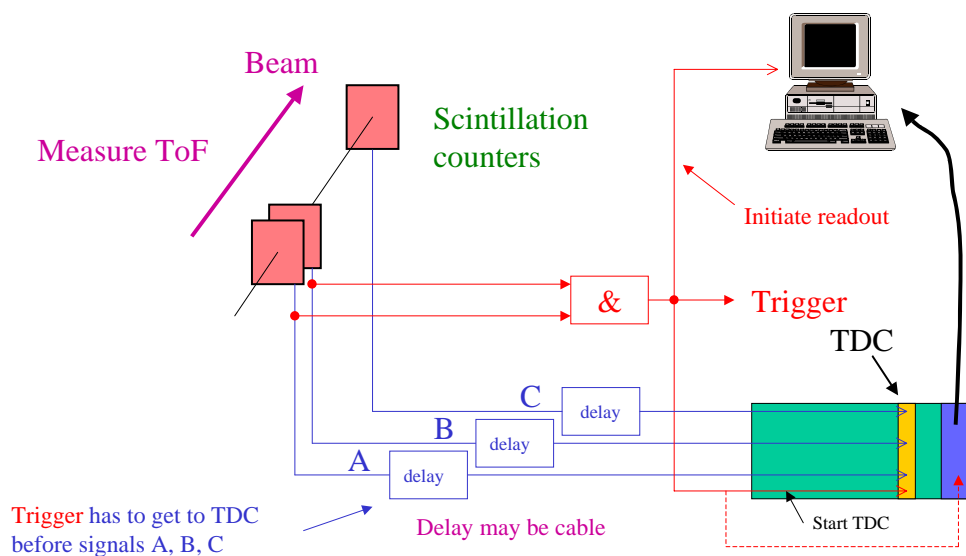


Fig. 1: Example of a simple experiment with its T/DAQ system

The ‘readout model’ of this traditional approach to T/DAQ is illustrated in Fig. 2, which shows the sequence of actions — arrival of the trigger, arrival of the detector signals (followed by digitization and storage in a data register in the TDC), and readout into the DAQ computer. Since no new trigger can be accepted until the readout is complete, the readout dead-time is given by the product of the trigger rate and the readout time.

²NIM [3] and CAMAC [4] modules are electronic modules that conform to agreed standards — modules for many functions needed in a T/DAQ system are available commercially.

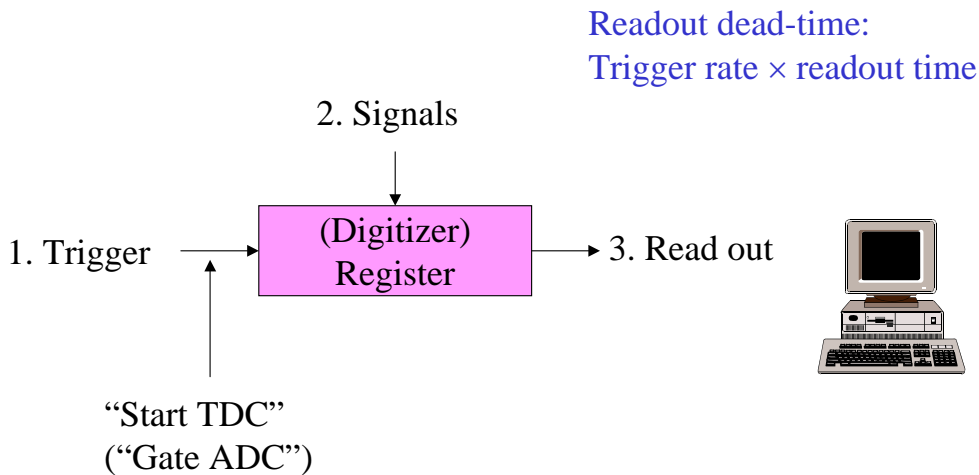


Fig. 2: Readout model in the ‘traditional’ approach

2.2 Local buffer

The traditional approach described above can be improved by adding a local ‘buffer’ memory into which the data are moved rapidly following a trigger, as illustrated in Fig. 3. This fast readout reduces the dead-time, which is now given by the product of the trigger rate and the local readout time. This approach is particularly useful in large systems, where the transfer of data can proceed in parallel with many local buffers (e.g., one local buffer for each crate of electronics) — local readout can remain fast even in a large system. Also, the data may be moved more quickly into the local buffer within the crate than into the DAQ computer. Note that the dashed line in the bottom, right-hand part of Fig. 1 indicates this extension to the traditional approach — the trigger signal is used to initiate the local readout within the crate.

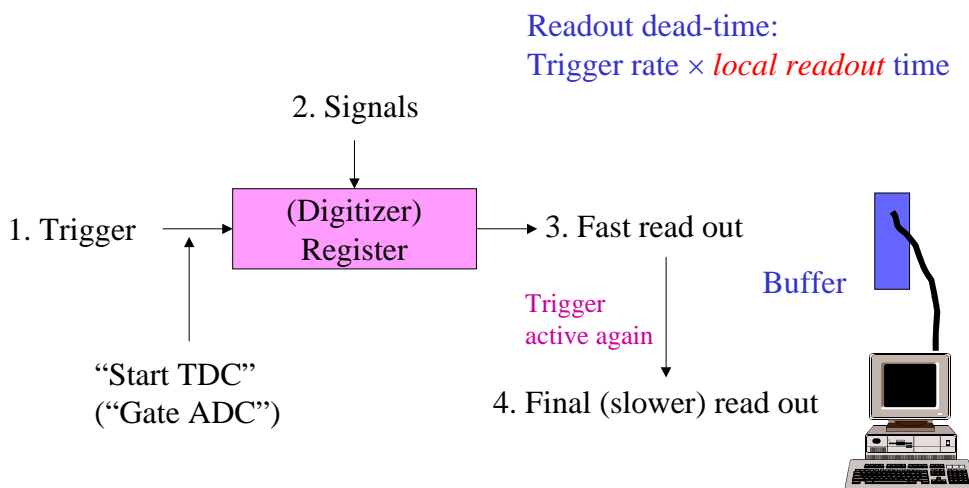


Fig. 3: Readout system with local buffer memory

The addition of a local buffer reduces the effective readout time, but the requirement of a fast trigger still remains. Signals have to be delayed until the trigger decision is available at the digitizers. This is not easy to achieve, even with very simple trigger logic — typically one relies on using fast (air-core) cables for trigger signals with the shortest possible routing so that the trigger signals arrive before the rest of the signals (which follow a longer routing on slower cables). It is not possible to apply complex selection criteria on this time-scale.

2.3 Multi-level triggers

It is not always possible to simultaneously meet the physics requirements (high efficiency, high background rejection) and achieve an extremely short trigger ‘latency’ (time to form the trigger decision and distribute it to the digitizers). A solution is to introduce the concept of multi-level triggers, where the first level has a short latency and maintains high efficiency, but only has a modest rejection power. Further background rejection comes from the higher trigger levels that can be slower. Sometimes the very fast first stage of the trigger is called the ‘pre-trigger’ — it may be sufficient to signal the presence of minimal activity in the detectors at this stage.

The use of a pre-trigger is illustrated in Fig. 4. Here the pre-trigger is used to provide the start signal to the TDCs (and to gate ADCs, etc.), while the main trigger (which can come later and can therefore be based on more complex calculations) is used to initiate the readout. In cases where the pre-trigger is not confirmed by the main trigger, a ‘fast clear’ is used to re-activate the digitizers (TDCs, ADCs, etc.).

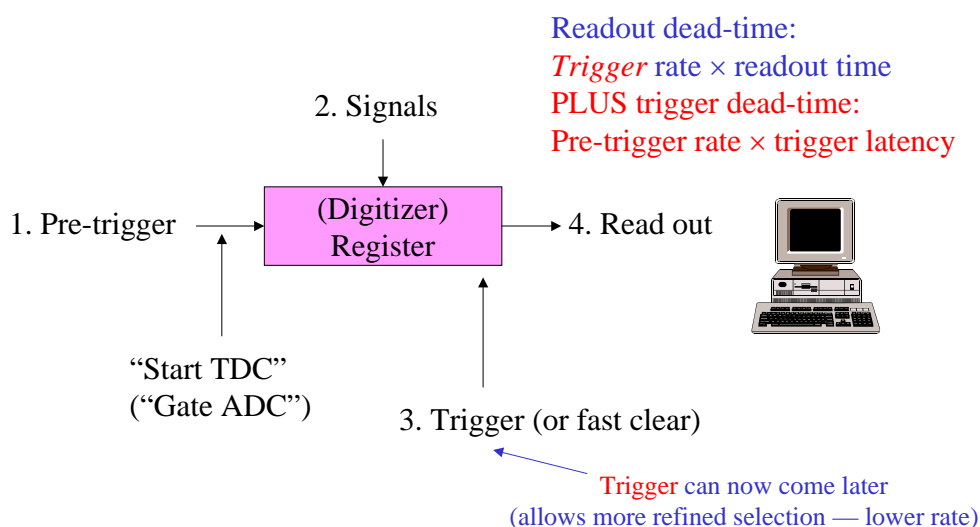


Fig. 4: Readout system with pre-trigger and fast clear

Using a pre-trigger (but without using a local buffer for now), the dead-time has two components. Following each pre-trigger there is a dead period until the trigger or fast clear is issued (defined here as the trigger latency). For the subset of pre-triggers that give rise to a trigger, there is an additional dead period given by the readout time. Hence, the total dead-time is given by the product of the pre-trigger rate and the trigger latency, added to the product of the trigger rate and the readout time.

The two ingredients — use of a local buffer and use of a pre-trigger with fast clear — can be combined as shown in Fig. 5, further reducing the dead-time. Here the total dead-time is given by the product of the pre-trigger rate and the trigger latency, added to the product of the trigger rate and the local readout time.

2.4 Further improvements

The idea of multi-level triggers can be extended beyond having two levels (pre-trigger and main trigger). One can have a series of trigger levels that progressively reduce the rate. The efficiency for the desired physics must be kept high at all levels since rejected events are lost forever. The initial levels can have modest rejection power, but they must be fast since they see a high input rate. The final levels must have strong rejection power, but they can be slower because they see a much lower rate (thanks to the rejection from the earlier levels).

In a multi-level trigger system, the total dead-time can be written as the sum of two parts: the trigger dead-time summed over trigger levels, and the readout dead-time. For a system with N levels, this can be written

$$\left(\sum_{i=2}^N R_{i-1} \times L_i\right) + R_N \times T_{\text{LRO}}$$

where R_i is the rate after the i^{th} trigger level, L_i is the latency of the i^{th} trigger level, and T_{LRO} is the local readout time. Note that R_1 corresponds to the pre-trigger rate.

In the above, two implicit assumptions have been made: (1) that all trigger levels are completed before the readout starts, and (2) that the pre-trigger (i.e., the lowest-level trigger) is available by the time the first signals from the detector arrive at the digitizers. The first assumption results in a long dead period for some events — those that survive the first (fast) levels of selection. The dead-time can be reduced by moving the data into intermediate storage after the initial stages of trigger selection, after which further low-level triggers can be accepted (in parallel with the execution of the later stages of trigger selection on the first event). The second assumption can also be avoided, e.g., in collider experiments with bunched beams as discussed below.

In the next section, aspects of particle colliders that affect the design of T/DAQ systems are introduced. Afterwards, the discussion returns to readout models and dead-time, considering the example of LEP experiments.

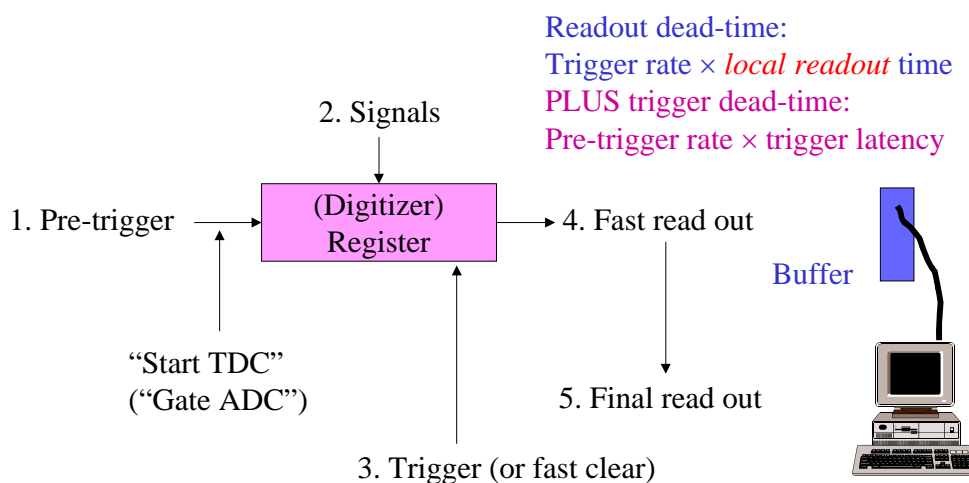


Fig. 5: Readout system using both pre-trigger and local buffer

3 Collider experiments

In high-energy particle colliders (HERA, LEP, LHC, Tevatron), the particles in the counter-rotating beams are bunched. Bunches of particles cross at regular intervals and interactions occur only during the bunch crossings. Here the trigger has the job of selecting the *bunch crossings* of interest for physics analysis, i.e., those containing interactions of interest.

In the following notes, the term ‘event’ is used to refer to the record of all the products from a given bunch crossing (plus any activity from other bunch crossings that gets recorded along with this). Be aware (and beware!) — the term ‘event’ is not uniquely defined! Some people use the term ‘event’ for the products of a single interaction between incident particles. Note that many people use ‘event’ interchangeably to mean different things.

In $e^+ e^-$ colliders, the interaction rate is very small compared to the bunch-crossing rate (because of the low $e^+ e^-$ cross-section). Generally, selected events contain just one interaction — i.e., the event

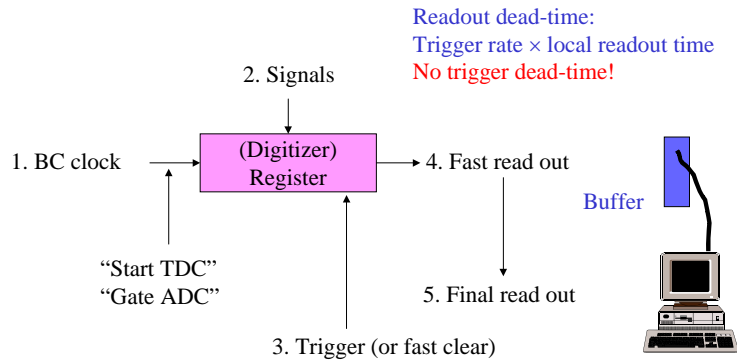


Fig. 6: Readout system using bunch-crossing (BC) clock and fast clear

is generally a single interaction. This was the case at LEP and also at the e - p collider HERA. In contrast, at LHC with the design luminosity \mathcal{L} of $10^{34} \text{ cm}^{-2} \text{ s}^{-1}$ for proton beams, each bunch crossing will contain on average about 25 interactions as discussed below. This means that an interaction of interest, e.g., one that produced $H \rightarrow ZZ \rightarrow e^+e^-e^+e^-$, will be recorded together with 25 other proton-proton interactions that occurred in the same bunch crossing. The interactions that make up the ‘underlying event’ are often called ‘minimum-bias’ interactions because they are the ones that would be selected by a trigger that selects interactions in an unbiased way. The presence of additional interactions that are recorded together with the one of interest is sometimes referred to as ‘pile-up’.

A further complication is that particle detectors do not have an infinitely fast response time — this is analogous to the exposure time of a camera. If the ‘exposure time’ is shorter than the bunch-crossing period, the event will contain only information from the selected bunch crossing. Otherwise, the event will contain, in addition, any activity from neighbouring bunches. In e^+e^- colliders (e.g., LEP) it is very unlikely for there to be any activity in nearby bunch crossings, which allows the use of slow detectors such as the time projection chamber (TPC). This is also true at HERA and in the ALICE experiment [5] at LHC that will study heavy-ion collisions at much lower luminosities than in the proton-proton case.

The bunch-crossing period for proton-proton collisions at LHC will be only 25 ns (corresponding to a 40 MHz rate). At the design luminosity the interaction rate will be $\mathcal{O}(10^9)$ Hz and, even with the short bunch-crossing period, there will be an average of about 25 interactions per bunch crossing. Some detectors, for example the ATLAS silicon tracker, achieve an exposure time of less than 25 ns, but many do not. For example, pulses from the ATLAS liquid-argon calorimeter extend over many bunch crossings.

The instrumentation for the LHC experiments is described in the lecture notes of Jordan Nash from this School [6]. The Particle Data Group’s Review of Particle Physics [7] includes much useful information, including summaries of the parameters of various particle colliders.

4 Design of a trigger and data-acquisition system for LEP

Let us now return to the discussion of designing a T/DAQ system, considering the case of experiments at LEP (ALEPH [8], DELPHI [9], L3 [10], and OPAL [11]), and building on the model developed in Section 2.

4.1 Using the bunch-crossing signal as a ‘pre-trigger’

If the time between bunch crossings (BCs) is reasonably long, one can use the clock that signals when bunches of particles cross as the pre-trigger. The first-level trigger can then use the time between bunch crossings to make a decision, as shown in Fig. 6. For most crossings the trigger will reject the event by issuing a fast clear — in such cases no dead-time is introduced. Following an ‘accept’ signal, dead-time

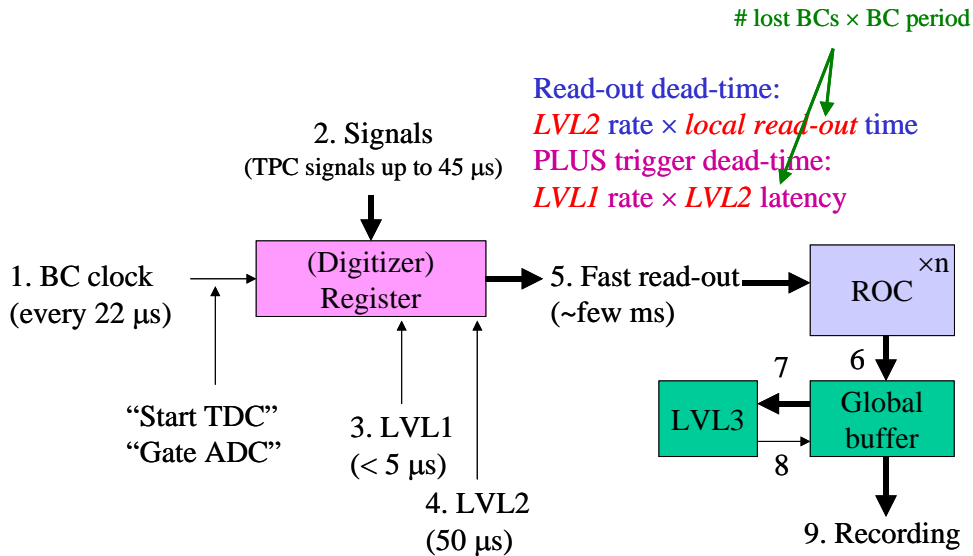


Fig. 7: LEP readout model (ALEPH)

will be introduced until the data have been read out (or until the event has been rejected by a higher-level trigger). This is the basis of the model that was used at LEP, where the bunch-crossing interval of 22 μs (11 μs in eight-bunch mode) allowed comparatively complicated trigger processing (latency of a few microseconds). Note that there is no first-level trigger dead-time because the decision is made during the interval between bunch crossings where no interactions occur. As discussed below, the trigger rates were reasonably low (very much less than the BC rate), giving acceptable dead-time due to the second-level trigger latency and the readout.

In the following, the readout model used at LEP is illustrated by concentrating on the example of ALEPH [8]³. Figure 7 shows the readout model, using the same kind of block diagram as presented in Section 2. The BC clock is used to start the TDCs and generate the gate for the ADCs, and a first-level (LVL1) trigger decision arrives in less than 5 μs so that the fast clear can be completed prior to the next bunch crossing. For events retained by LVL1, a more sophisticated second-level (LVL2) trigger decision is made after a total of about 50 μs. Events retained by LVL2 are read out to local buffer memory (within the readout controllers or ‘ROCs’), and then passed to a global buffer. There is a final level of selection (LVL3) before recording the data on permanent storage for offline analysis.

For readout systems of the type shown in Fig. 7, the total dead-time is given by the sum of two components — the trigger dead-time and the readout dead-time.

The trigger dead-time is evaluated by counting the number of BCs that are lost following each LVL1 trigger, then calculating the product of the LVL1 trigger rate, the number of lost BCs and the BC period. Note that the effective LVL2 latency, given by the number of lost BCs and the BC period, is less than (or equal to) the true LVL2 latency.

The readout dead-time is given by the product of the LVL2 trigger rate and the time taken to perform local readout into the ROCs. Strictly speaking, one should also express this dead-time in terms of the number of BCs lost after the LVL2 trigger, but since the readout time is much longer than the BC period the difference is unimportant. Note that, as long as the buffers in the ROCs and the global buffers do not fill up, no additional dead-time is introduced by the final readout and the LVL3 trigger.

Let us now look quantitatively at the example of the DELPHI experiment for which the T/DAQ

³The author was not involved in any of the LEP experiments. In these lectures the example of ALEPH is used to illustrate how triggers and data acquisition were implemented at LEP; some numbers from DELPHI are also presented. The T/DAQ systems in all of the LEP experiments were conceptually similar.

Table 1: Typical T/DAQ parameters for the DELPHI experiment at LEP-II

Quantity	Value
LVL1 rate	$\sim 500\text{--}1000$ Hz (instrumental background)
LVL2 rate	6–8 Hz
LVL3 rate	4–6 Hz
LVL2 latency	38 μs (1 lost BC \Rightarrow 22 μs effective)
Local readout time	~ 2.5 ms
Readout dead-time	~ 7 Hz $\times 2.5 \cdot 10^{-3}$ s = 1.8%
Trigger dead-time	~ 750 Hz $\times 22 \cdot 10^{-6}$ s = 1.7%
Total dead-time	$\sim 3\text{--}4\%$

system was similar to that described above for ALEPH. Typical numbers for LEP-II⁴ are shown in Table 1 [9].

4.2 Data acquisition at LEP

Let us now continue our examination of the example of the ALEPH T/DAQ system. Following a LVL2 trigger, events were read out locally and in parallel within the many readout crates — once the data had been transferred within each crate to the ROC, further LVL1 and LVL2 triggers could be accepted. Subsequently, the data from the readout crates were collected by the main readout computer, ‘building’ a complete event. As shown in Fig. 8, event building was performed in two stages: an event contained a number of sub-events, each of which was composed of several ROC data blocks. Once a complete event was in the main readout computer, the LVL3 trigger made a final selection before the data were recorded.

The DAQ system used a hierarchy of computers — the local ROCs in each crate; event builders (EBs) for sub-events; the main EB; the main readout computer. The ROCs performed some data processing (e.g., applying calibration algorithms to convert ADC values to energies) in addition to reading out the data from ADCs, TDCs, etc. (Zero suppression was already performed at the level of the digitizers where appropriate.) The first layer of EBs combined data read out from the ROCs of individual sub-detectors into sub-events; then the main EB combined the sub-events for the different sub-detectors. Finally, the main readout computer received full events from the main EB, performed the LVL3 trigger selection, and recorded selected events for subsequent analysis.

As indicated in Fig. 9, event building was bus based — each ROC collected data over a bus from the digitizing electronics; each sub-detector EB collected data from several ROCs over a bus; the main EB collected data from the sub-detector EBs over a bus. As a consequence, the main EB and the main readout computer saw the full data rate prior to the final LVL3 selection. At LEP this was fine — with an event rate after LVL2 of a few hertz and an event size of 100 kbytes, the data rate was a few hundred kilobytes per second, much less than the available bandwidth (e.g., 40 Mbytes/s maximum on VME bus [12]).

4.3 Triggers at LEP

The triggers at LEP aimed to select any $e^+ e^-$ annihilation event with a visible final state, including events with little visible energy, plus some fraction of two-photon events, plus Bhabha scattering events. Furthermore, they aimed to select most events by multiple, independent signatures so as to maximize the trigger efficiency and to allow the measurement of the efficiency from the data. The probability for an event to pass trigger A or trigger B is $\sim 1 - \delta_A \delta_B$, where δ_A and δ_B are the individual trigger inefficiencies, which is very close to unity for small δ . Starting from a sample of events selected with trigger A, the

⁴LEP-II refers to the period when LEP operated at high energy, after the upgrade of the RF system.

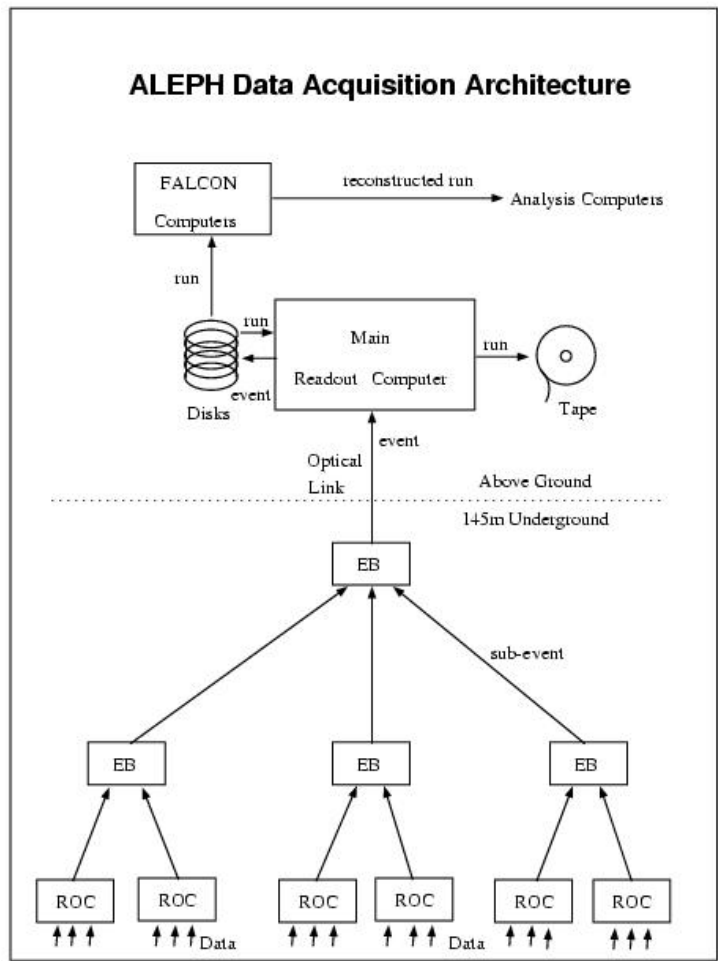


Fig. 8: ALEPH data-acquisition architecture

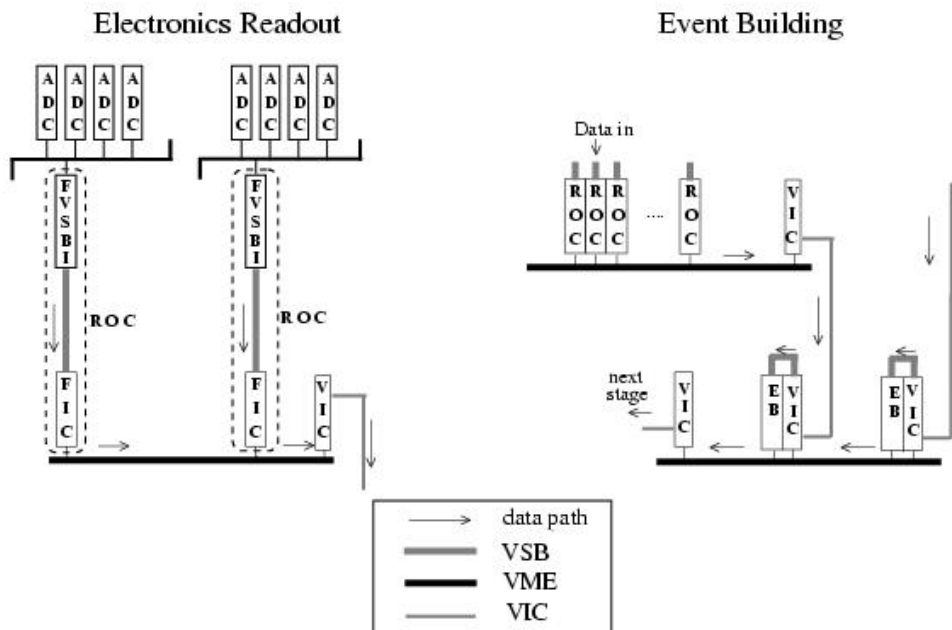


Fig. 9: Event building in ALEPH

efficiency of trigger B can be estimated as the fraction of events passing trigger B in addition. Note that in the actual calculations small corrections were applied for correlations between the trigger efficiencies.

5 Towards the LHC

In some experiments it is not practical to make a trigger in the time between bunch crossings because of the short BC period—the BC interval is 396 ns at Tevatron-II⁵, 96 ns at HERA and 25 ns at LHC. In such cases the concept of ‘pipelined’ readout has to be introduced (also pipelined LVL1 trigger processing). Furthermore, in experiments at high-luminosity hadron colliders the data rates after the LVL1 trigger selection are very high, and new ideas have to be introduced for the high-level triggers (HLT) and DAQ—in particular, event building has to be based on data networks and switches rather than data buses.

5.1 Pipelined readout

In pipelined readout systems (see Fig. 10), the information from each BC, for each detector element, is retained during the latency of the LVL1 trigger (several μ s). The information may be retained in several forms— analog levels (held on capacitors); digital values (e.g., ADC results); binary values (i.e., hit or no hit). This is done using a logical ‘pipeline’, which may be implemented using a first-in, first-out (FIFO) memory circuit. Data reaching the end of the pipeline are either discarded or, in the case of a trigger accept decision, moved to a secondary buffer memory (small fraction of BCs).

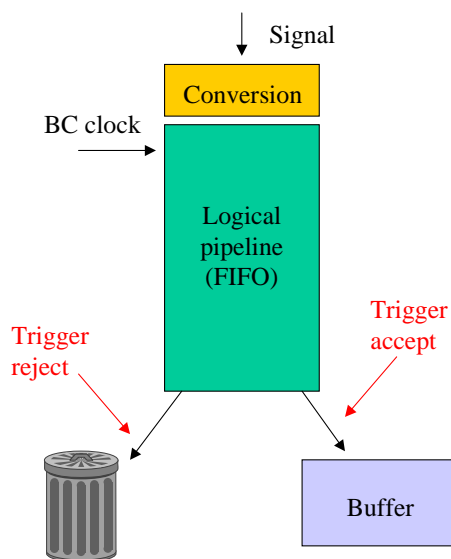


Fig. 10: Example of pipelined readout

Pipelined readout systems will be used in the LHC experiments (they have already been used in experiments at HERA [13, 14] and the Tevatron [15, 16], but the demands at LHC are even greater because of the short BC period). A typical LHC pipelined readout system is illustrated in Fig. 11, where the digitizer and pipeline are driven by the 40 MHz BC clock. A LVL1 trigger decision is made for each bunch crossing (i.e., every 25 ns), although the LVL1 latency is several microseconds—the LVL1 trigger must concurrently process many events (this is achieved by using pipelined trigger processing as discussed below).

The data for events that are selected by the LVL1 trigger are transferred into a ‘derandomizer’—a memory that can accept the high instantaneous input rate (i.e., one word per 25 ns) while being read out

⁵Tevatron-II refers to the Tevatron collider after the luminosity upgrade.

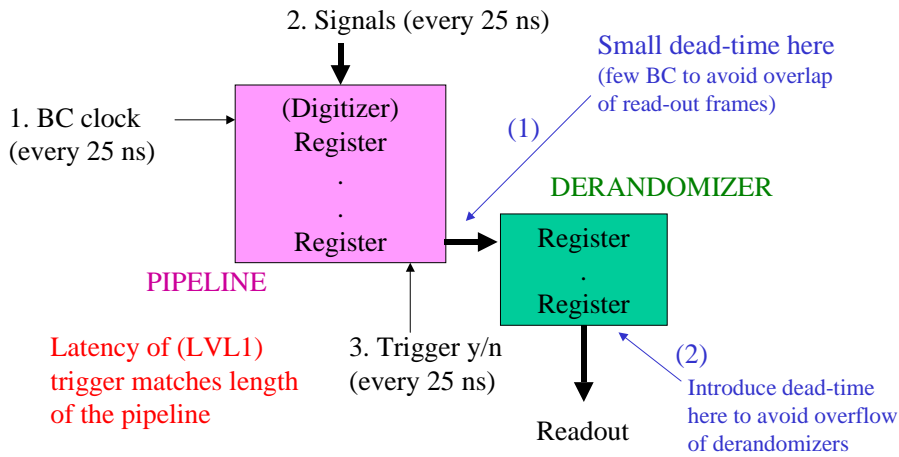


Fig. 11: Pipelined readout with derandomizer at the LHC

at the much lower average data rate (determined by the LVL1 trigger rate rather than the BC rate). In principle no dead-time needs to be introduced in such a system. However, in practice, data are retained for a few BCs around the one that gave rise to the trigger, and a dead period of a few BCs is introduced to ensure that the same data do not have to be accessed for more than one trigger. Dead-time must also be introduced to prevent the derandomizers from overflowing, e.g., where, due to a statistical fluctuation, many LVL1 triggers arrive in quick succession. The dead-time from the first of these sources can be estimated as follows (numbers from ATLAS): taking a LVL1 trigger rate of 75 kHz and 4 dead BCs following each LVL1 trigger gives $75 \text{ kHz} \times 4 \times 25 \text{ ns} = 0.75\%$. The dead-time from the second source depends on the size of the derandomizer and the speed with which it can be emptied—in ATLAS the requirements are $< 1\%$ dead-time for a LVL1 rate of 75 kHz ($< 6\%$ for 100 kHz).

Some of the elements of the readout chain in the LHC experiments have to be mounted on the detectors (and hence are totally inaccessible during running of the machine and are in an environment with high radiation levels). This is shown for the case of CMS in Fig. 12.

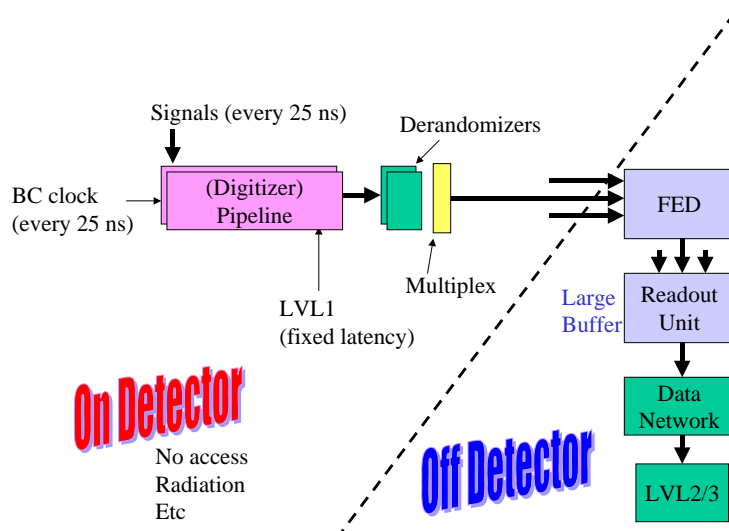


Fig. 12: Location of readout components in CMS

There are a variety of options for the placement of digitization in the readout chain, and the optimum choice depends on the characteristics of the detector in question. Digitization may be performed on

the detector at 40 MHz rate, prior to a digital pipeline (e.g., CMS calorimeter). Alternatively, it may be done on the detector after multiplexing signals from several analog pipelines (e.g., ATLAS EM calorimeter) — here the digitization rate can be lower, given by the LVL1 trigger rate multiplied by the number of signals to be digitized per trigger. Another alternative (e.g., CMS tracker) is to multiplex analog signals from the pipelines over analog links, and then to perform the digitization off-detector.

5.2 Pipelined LVL1 trigger

As discussed above, the LVL1 trigger has to deliver a new decision every BC, although the trigger latency is much longer than the BC period; the LVL1 trigger must concurrently process many events. This can be achieved by ‘pipelining’ the processing in custom trigger processors built using modern digital electronics. The key ingredients in this approach are to break the processing down into a series of steps, each of which can be performed within a single BC period, and to perform many operations in parallel by having separate processing logic for each calculation. Note that in such a system the latency of the LVL1 trigger is fixed — it is determined by the number of steps in the calculation, plus the time taken to move signals and data to, from and between the components of the trigger system (e.g., propagation delays on cables).

Pipelined trigger processing is illustrated in Fig. 13 — as will be seen later, this example corresponds to a (very small) part of the ATLAS LVL1 calorimeter trigger processor. The drawing on the left of Fig. 13 depicts the EM calorimeter as a grid of ‘towers’ in η - ϕ space (η is pseudorapidity, ϕ is azimuth angle). The logic shown on the right determines if the energy deposited in a horizontal or vertical pair of towers in the region [A, B, C] exceeds a threshold. In each 25 ns period, data from one layer of ‘latches’ (memory registers) are processed through the next step in the processing ‘pipe’, and the results are captured in the next layer of latches. Note that, in the real system, such logic has to be performed in parallel for ~ 3500 positions of the reference tower; the tower ‘A’ could be at any position in the calorimeter. In practice, modern electronics is capable of doing more than a simple add or compare operation in 25 ns, so there is more logic between the latches than in this illustration.

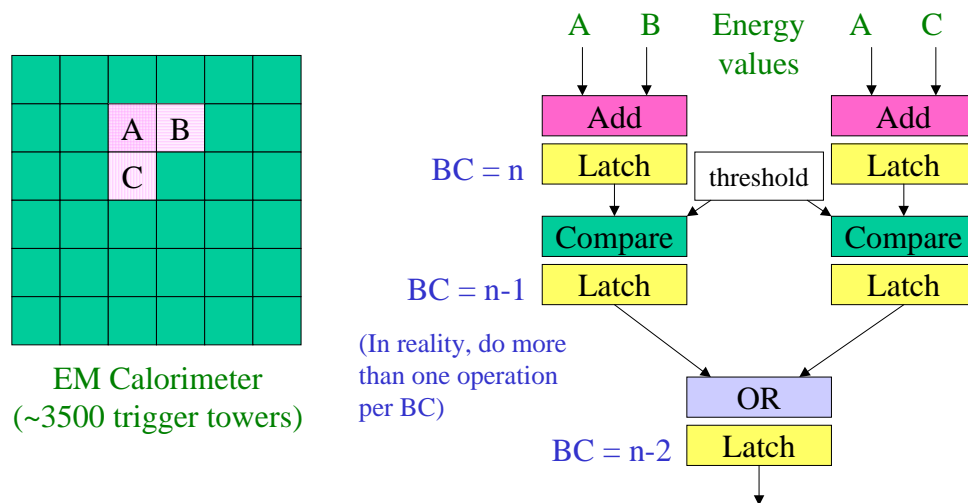


Fig. 13: Illustration of pipelined processing

The amount of data to be handled varies with depth in the processing pipeline, as indicated in Fig. 14. Initially the amount of data expands compared to the raw digitization level since each datum typically participates in several operations — the input data need to be ‘fanned out’ to several processing elements. Subsequently the amount of data decreases as one moves further down the processing tree. The final trigger decision can be represented by a single bit of information for each BC — yes or no (binary 1 or 0). Note that, in addition to the trigger decision, the LVL1 processors produce a lot of data

for use in monitoring the system and to guide the higher levels of selection.

Although they have not been discussed in these lectures because of time limitations, some fixed-target experiments have very challenging T/DAQ requirements. Some examples can be found in Refs. [17, 18].

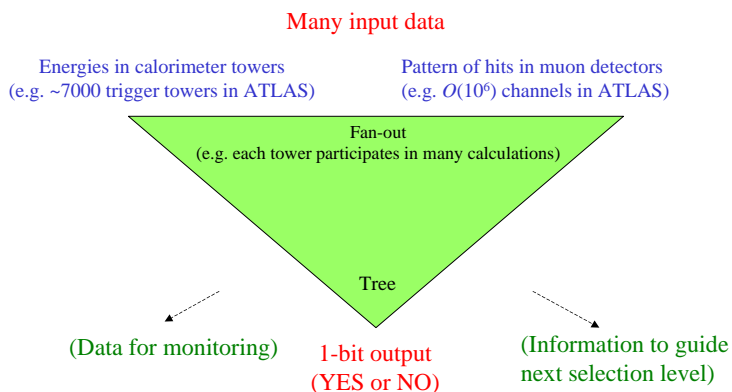


Fig. 14: LVL1 data flow

6 High-level triggers and data acquisition at the LHC

In the LHC experiments, data are transferred after a LVL1 trigger accept decision to large buffer memories — in normal operation the subsequent stages should not introduce further dead-time. At this point in the readout chain, the data rates are still massive. An event size of ~ 1 Mbyte (after zero suppression or data compression) at ~ 100 kHz event rate gives a total bandwidth of ~ 100 Gbytes/s (i.e., ~ 800 Gbits/s). This is far beyond the capacity of the bus-based event building of LEP. Such high data rates will be dealt with by using network-based event building and by only moving a subset of the data.

Network-based event building is illustrated in Fig. 15 for the example of CMS. Data are stored in the readout systems until they have been transferred to the filter systems [associated with high-level trigger (HLT) processing], or until the event is rejected. Note that no node in the system sees the full data rate — each readout system covers only a part of the detector and each filter system deals with only a fraction of the events.

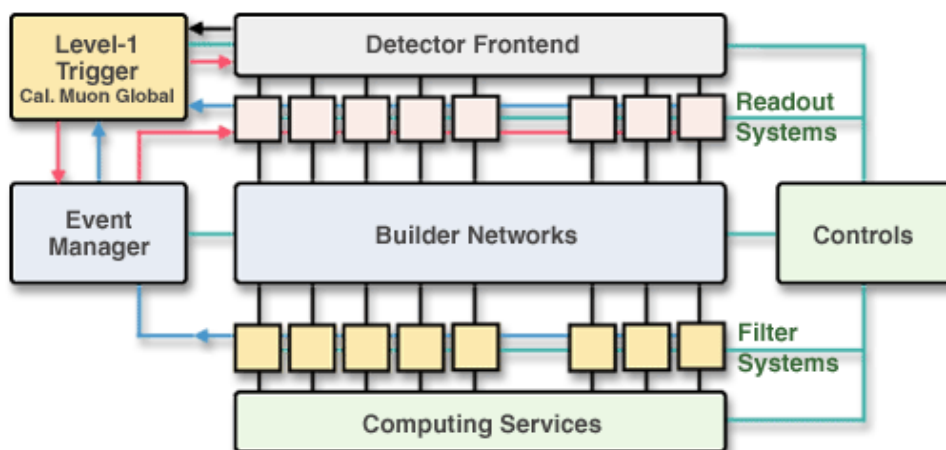


Fig. 15: CMS event builder

The LVL2 trigger decision can be made without accessing or processing all of the data. Substantial rejection can be made with respect to LVL1 without accessing the inner-tracking detectors — calorimeter

triggers can be refined using the full-precision, full-granularity calorimeter information; muon triggers can be refined using the high-precision readout from the muon detectors. It is therefore only necessary to access the inner-tracking data for the subset of events that pass this initial selection. ATLAS and CMS both use this sequential selection strategy. Nevertheless, the massive data rates pose problems even for network-based event building, and different solutions have been adopted in ATLAS and CMS to address this.

In CMS the event building is factorized into a number of ‘slices’, each of which sees only a fraction of the total rate (see Fig. 16). This still requires a large total network bandwidth (which has implications for the cost), but it avoids the need for a very big central network switch. An additional advantage of this approach is that the size of the system can be scaled, starting with a few slices and adding more later (e.g., as additional funding becomes available).

Eight slices:
Each slice sees
only 1/8th of
the events

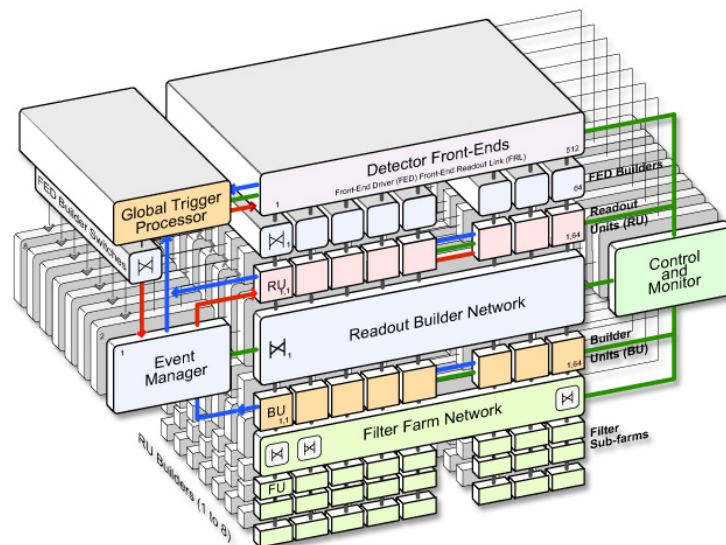


Fig. 16: The CMS slicing concept

In ATLAS the amount of data to be moved is reduced by using the region-of-interest (RoI) mechanism (see Fig. 17). Here, the LVL1 trigger indicates the geographical location in the detector of candidate objects. LVL2 then only needs to access data from the RoIs, a small fraction of the total, even for the calorimeter and muon detectors that participated in the LVL1 selection. This requires relatively complicated mechanisms to serve the data selectively to the LVL2 trigger processors.

In the example shown in Fig. 17, two muons are identified by LVL1. It can be seen that only a small fraction of the detector has to be accessed to validate the muons. In a first step only the data from the muon detectors are accessed and processed, and many events will be rejected where the more detailed analysis does not confirm the comparatively crude LVL1 selection (e.g., sharper p_T cut). For those events that remain, the inner-tracker data will be accessed within the RoIs, allowing further rejection (e.g., of muons from decays in flight of charged pions and kaons). In a last step, calorimeter information may be accessed within the RoIs to select isolated muons (e.g., to reduce the high rate of events with muons from bottom and charm decays, while retaining those from W and Z decays).

Concerning hardware implementation, the computer industry is putting on the market technologies that can be used to build much of the HLT/DAQ systems at the LHC. Computer network products now offer high performance at affordable cost. Personal computers (PCs) provide exceptional value for money in processing power, with high-speed network interfaces as standard items. Nevertheless, custom hardware is needed in the parts of the system that see the full LVL1 trigger output rate (~ 100 kHz). This concerns the readout systems that receive the detector data following a positive LVL1 trigger decision,

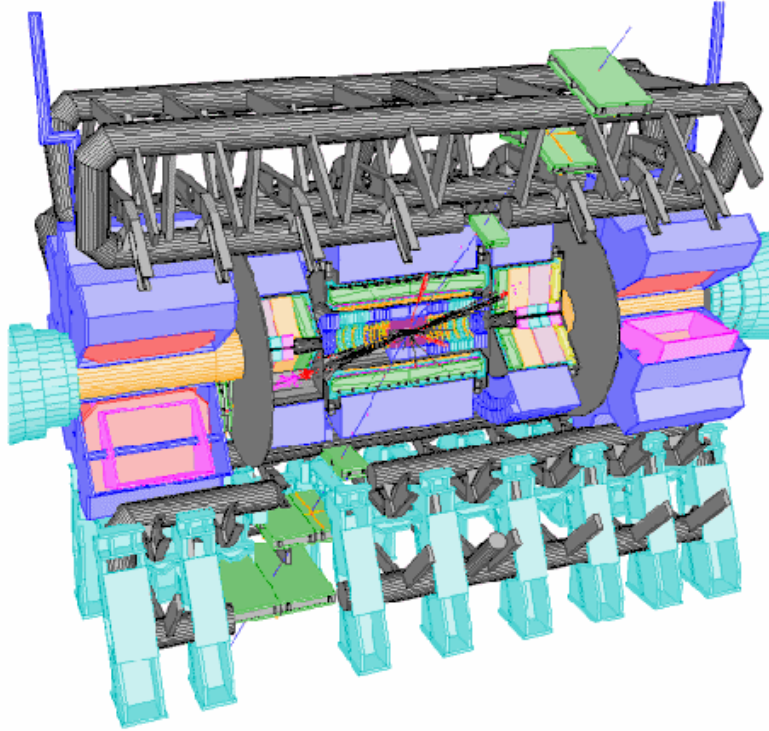


Fig. 17: The ATLAS region-of-interest concept — example of a dimuon event (see text)

and (in ATLAS) the interface to the LVL1 trigger that receives the RoI pointers. Of course, this is in addition to the specialized front-end electronics associated with the detectors that was discussed earlier (digitization, pipelines, derandomizers, etc.).

7 Physics requirements — two examples

In the following, the physics requirements on the T/DAQ systems at LEP and at the LHC are examined. These are complementary cases — at LEP precision physics was the main emphasis, at the LHC discovery physics will be the main issue. Precision physics at LEP needed accurate determination of the absolute cross-section (e.g., in the determination of the number of light-neutrino species). Discovery physics at the LHC will require sensitivity to a huge range of predicted processes with diverse signatures (with very low signal rates expected in some cases), aiming to be as sensitive as possible to new physics that has not been predicted (by using inclusive signatures). This has to be achieved in the presence of an enormous rate of Standard Model physics backgrounds (the rate of proton–proton collisions at the LHC will be $\mathcal{O}(10^9)$ Hz — $\sigma \sim 100$ mb, $\mathcal{L} \sim 10^{34}$ cm⁻² s⁻¹).

7.1 Physics requirements at LEP

Triggers at LEP aimed to identify all events coming from e^+e^- annihilations with visible final states. At LEP-I, operating with $\sqrt{s} \sim m_Z$, this included $Z \rightarrow$ hadrons, $Z \rightarrow e^+e^-$, $Z \rightarrow \mu^+\mu^-$, and $Z \rightarrow \tau^+\tau^-$; at LEP-II, operating above the WW threshold, this included WW, ZZ and single-boson events. Sensitivity was required even in cases where there was little visible energy, e.g., in the Standard Model for $e^+e^- \rightarrow Z\gamma$, with $Z \rightarrow \nu\nu$, and in new-particle searches such as $e^+e^- \rightarrow \tilde{\chi}^+\tilde{\chi}^-$ for the case of small $\tilde{\chi}^\pm - \tilde{\chi}^0$ mass difference that gives only low-energy visible particles ($\tilde{\chi}^0$ is the lightest supersymmetric particle). In addition, the triggers had to retain some fraction of two-photon collision events (used for QCD studies), and identify Bhabha scatters (needed for precise luminosity determination).

The triggers could retain events with any significant activity in the detector. Even when running at

the Z peak, the rate of Z decays was only $\mathcal{O}(1)$ Hz — physics rate was not an issue. The challenge was in maximizing the efficiency (and acceptance) of the trigger, and making sure that the small inefficiencies were very well understood. The determination of absolute cross-section depends on knowing the integrated luminosity and the experimental efficiency to select the process in question (i.e., the efficiency to trigger on the specific physics process). Precise determination of the integrated luminosity required excellent understanding of the trigger efficiency for Bhabha-scattering events (luminosity determined from the rate of Bhabha scatters within a given angular range). A major achievement at LEP was to reach ‘per mil’ precision.

The trigger rates (events per second) and the DAQ rates (bytes per second) at LEP were modest as discussed in Section 4.

7.2 Physics requirements at the LHC

Triggers in the general-purpose proton–proton experiments at the LHC (ATLAS [19, 20] and CMS [21, 22]) will have to retain as high as possible a fraction of the events of interest for the diverse physics programmes of these experiments. Higgs searches in and beyond the Standard Model will include looking for $H \rightarrow ZZ \rightarrow \text{leptons}$ and also $H \rightarrow b\bar{b}$. Supersymmetry (SUSY) searches will be performed with and without the assumption of R-parity conservation. One will search for other new physics using inclusive triggers that one hopes will be sensitive to unpredicted processes. In parallel with the searches for new physics, the LHC experiments aim to do precision physics, such as measuring the W mass and some B-physics studies, especially in the early phases of LHC running when the luminosity is expected to be comparatively low.

In contrast to the experiments at LEP, the LHC trigger systems have a hard job to reduce the physics event rate to a manageable level for data recording and offline analysis. As discussed above, the design luminosity $\mathcal{L} \sim 10^{34} \text{ cm}^{-2} \text{ s}^{-1}$, together with $\sigma \sim 100 \text{ mb}$, implies an $\mathcal{O}(10^9)$ Hz interaction rate. Even the rate of events containing leptonic decays of W and Z bosons is $\mathcal{O}(100)$ Hz. Furthermore, the size of the events is very large, $\mathcal{O}(1)$ Mbyte, reflecting the huge number of detector channels and the high particle multiplicity in each event. Recording and subsequently processing offline $\mathcal{O}(100)$ Hz event rate per experiment with an $\mathcal{O}(1)$ Mbyte event size is considered feasible, but it implies major computing resources [23]. Hence, only a tiny fraction of proton–proton collisions can be selected — taking the order-of-magnitude numbers given above, the maximum fraction of interactions that can be selected is $\mathcal{O}(10^{-7})$. Note that the general-purpose LHC experiments have to balance the needs of maximizing physics coverage and reaching acceptable (i.e., affordable) recording rates.

The LHCb experiment [24], which is dedicated to studying B-physics, faces similar challenges to ATLAS and CMS. It will operate at a comparatively low luminosity ($\mathcal{L} \sim 10^{32} \text{ cm}^{-2} \text{ s}^{-1}$), giving an overall proton–proton interaction rate of $\sim 20 \text{ MHz}$ — chosen to maximize the rate of single-interaction bunch crossings. The event size will be comparatively small ($\sim 100 \text{ kbytes}$) as a result of having fewer detector channels and of the lower occupancy of the detector (due to the lower luminosity with less pile-up). However, there will be a very high rate of beauty production in LHCb — taking $\sigma \sim 500 \text{ } \mu\text{b}$, the production rate will be $\sim 100 \text{ kHz}$ — and the trigger must search for specific B-decay modes that are of interest for physics analysis, with the aim of recording an event rate of only $\sim 200 \text{ Hz}$.

The heavy-ion experiment ALICE [5] is also very demanding, particularly from the DAQ point of view. The total interaction rate will be much smaller than in the proton–proton experiments — $\mathcal{L} \sim 10^{27} \text{ cm}^{-2} \text{ s}^{-1}$ is predicted to give a rate $\sim 8000 \text{ Hz}$ for Pb–Pb collisions. However, the event size will be huge due to the high final-state multiplicity in Pb–Pb interactions at LHC energy. Up to $\mathcal{O}(10^4)$ charged particles will be produced in the central region, giving an event size of up to $\sim 40 \text{ Mbytes}$ when the full detector is read out. The ALICE trigger will select ‘minimum-bias’ and ‘central’ events (rates scaled down to a total of about 40 Hz), and events with dileptons ($\sim 1 \text{ kHz}$ with only part of the detector read out). Even compared to the other LHC experiments, the volume of data to be stored and subsequently processed offline will be massive, with a data rate to storage of $\sim 1 \text{ Gbytes/s}$ (considered to be

about the maximum affordable rate).

8 Signatures of different types of particle

The generic signatures for different types of particle are illustrated in Fig. 18. Moving away from the interaction point (shown as a star on the left-hand side of Fig. 18), one finds the inner tracking detector (IDET), the electromagnetic calorimeter (ECAL), the hadronic calorimeter (HCAL) and the muon detectors (MuDET). Charged particles (electrons, muons and charged hadrons) leave tracks in the IDET. Electrons and photons shower in the ECAL, giving localized clusters of energy without activity in the HCAL. Hadrons produce larger showers that may start in the ECAL but extend into the HCAL. Muons traverse the calorimeters with minimal energy loss and are detected in the MuDET.

The momenta of charged particles are measured from the radii of curvature of their tracks in the IDET which is embedded in a magnetic field. A further measurement of the momenta of muons may be made in the MuDET using a second magnet system. The energies of electrons, photons and hadrons are measured in the calorimeters. Although neutrinos leave the detector system without interaction, one can infer their presence from the momentum imbalance in the event (sometimes referred to as ‘missing energy’). Hadronic jets contain a mixture of particles, including neutral pions that decay almost immediately into photon pairs that are then detected in the ECAL. The jets appear as broad clusters of energy in the calorimeters where the individual particles will sometimes not be resolved.

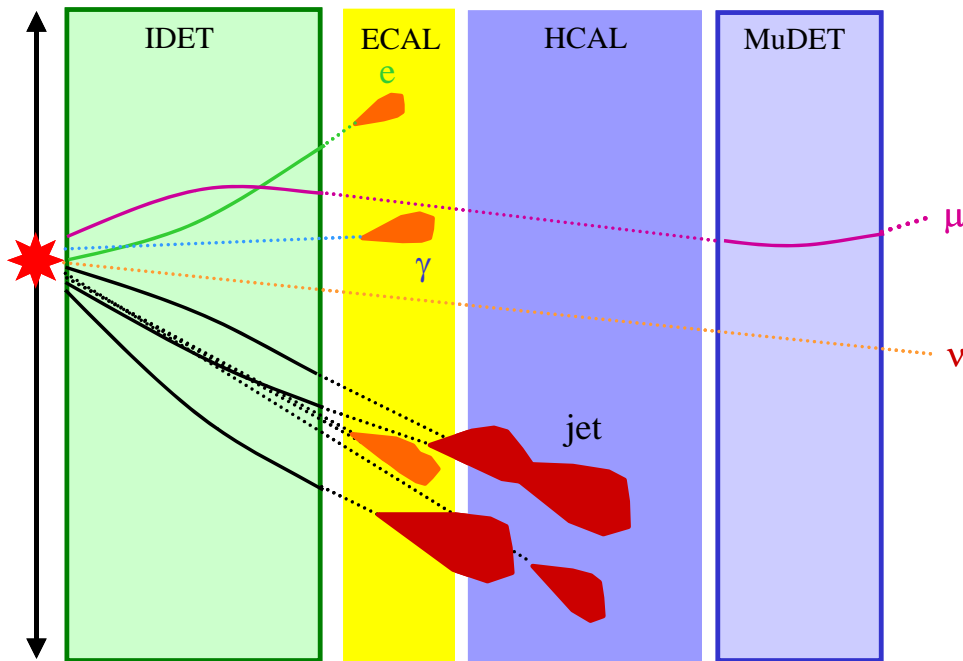


Fig. 18: Signatures of different types of particle in a generic detector

9 Selection criteria and trigger implementations at LEP

The details of the selection criteria and trigger implementations at LEP varied from experiment to experiment [8–11]. Discussion of the example of ALEPH is continued with the aim of giving a reasonably in-depth view of one system. For triggering purposes, the detector was divided into segments with a total of 60 regions in θ, ϕ (θ is polar angle and ϕ is azimuth with respect to the beam axis). Within these segments, the following trigger objects were identified:

1. muon — requiring a track penetrating the hadron calorimeter and seen in the inner tracker;

2. charged electromagnetic (EM) energy — requiring an EM calorimeter cluster and a track in the inner tracker;
3. neutral EM energy — requiring an EM calorimeter cluster (with higher thresholds than in (2) to limit the rate to acceptable levels).

In addition to the above local triggers, there were total-energy triggers (applying thresholds on energies summed over large regions—the barrel or a full endcap), a back-to-back tracks trigger, and triggers for Bhabha scattering (luminosity monitor).

The LVL1 triggers were implemented using a combination of analog and digital electronics. The calorimeter triggers were implemented using analog electronics to sum signals before applying thresholds on the sums. The LVL1 tracking trigger looked for patterns of hits in the inner-tracking chamber (ITC) consistent with a track with $p_T > 1$ GeV⁶—at LVL2 the Time Projection Chamber (TPC) was used instead. The final decision was made by combining digital information from calorimeter and tracking triggers, making local combinations within segments of the detector, and then making a global combination (logical OR of conditions).

10 Selection criteria at LHC

Features that distinguish new physics from the bulk of the cross-section for Standard Model processes at hadron colliders are generally the presence of high- p_T particles (or jets). For example, these may be the products of the decays of new heavy particles. In contrast, most of the particles produced in minimum-bias interactions are soft ($p_T \sim 1$ GeV or less). More specific signatures are the presence of high- p_T leptons (e, μ , τ), photons and/or neutrinos. For example, these may be the products (directly or indirectly) of new heavy particles. Charged leptons, photons and neutrinos give a particularly clean signature (c.f. low- p_T hadrons in minimum-bias events), especially if they are ‘isolated’ (i.e., not inside jets). The presence of heavy particles such as W and Z bosons can be another signature for new physics—e.g., they may be produced in Higgs decays. Leptonic W and Z decays give a very clean signature that can be used in the trigger. Of course it is interesting to study W and Z boson production *per se*, and such events can be very useful for detector studies (e.g., calibration of the EM calorimeters).

In view of the above, LVL1 triggers at hadron colliders search for the following signatures (see Fig. 18).

- High- p_T muons — these can be identified as charged particles that penetrate beyond the calorimeters; a p_T cut is needed to control the rate of muons from $\pi^\pm \rightarrow \mu^\pm \nu$ and $K^\pm \rightarrow \mu^\pm \nu$ decays in flight, as well as those from semi-muonic beauty and charm decays.
- High- p_T photons — these can be identified as narrow clusters in the EM calorimeter; cuts are made on transverse energy ($E_T > \text{threshold}$), and isolation and associated hadronic transverse energy ($E_T < \text{threshold}$), to reduce the rate due to misidentified high- p_T jets.
- High- p_T electrons — identified in a similar way to photons, although some experiments require a matching track as early as LVL1.
- High- p_T taus — identified as narrow clusters in the calorimeters (EM and hadronic energy combined).
- High- p_T jets — identified as wider clusters in the calorimeters (EM and hadronic energy combined); note that one needs to cut at very high p_T to get acceptable rates given that jets are the dominant high- p_T process.
- Large missing E_T or scalar E_T .

Some experiments also search for tracks from displaced secondary vertices at an early stage in the trigger selection.

⁶Here, p_T is transverse momentum (measured with respect to the beam axis); similarly, E_T is transverse energy.

The trigger selection criteria are typically expressed as a list of conditions that should be satisfied — if any of the conditions is met, a trigger is generated (subject to dead-time requirements, etc.). In these notes, the list of conditions is referred to as the ‘trigger menu’, although the name varies from experiment to experiment. An illustrative example of a LVL1 trigger menu for high-luminosity running at LHC includes the following (rates [19] are given for the case of ATLAS at $\mathcal{L} \sim 10^{34} \text{ cm}^{-2} \text{ s}^{-1}$):

- one or more muons with $p_T > 20 \text{ GeV}$ (rate $\sim 11 \text{ kHz}$);
- two or more muons each with $p_T > 6 \text{ GeV}$ (rate $\sim 1 \text{ kHz}$);
- one or more e/γ with $E_T > 30 \text{ GeV}$ (rate $\sim 22 \text{ kHz}$);
- two or more e/γ each with $E_T > 20 \text{ GeV}$ (rate $\sim 5 \text{ kHz}$);
- one or more jets with $E_T > 290 \text{ GeV}$ (rate $\sim 200 \text{ Hz}$);
- one or more jets with $E_T > 100 \text{ GeV}$ and missing- $E_T > 100 \text{ GeV}$ (rate $\sim 500 \text{ Hz}$);
- three or more jets with $E_T > 130 \text{ GeV}$ (rate $\sim 200 \text{ Hz}$);
- four or more jets with $E_T > 90 \text{ GeV}$ (rate $\sim 200 \text{ Hz}$).

The above list represents an extract from a LVL1 trigger menu, indicating some of the most important trigger requirements — the full menu would include many items in addition (typically more than 100 items in total). The additional items are expected to include the following:

- τ (or isolated single-hadron) candidates;
- combinations of objects of different types (e.g., muon *and* e/γ);
- pre-scaled⁷ triggers with lower thresholds;
- triggers needed for technical studies and to aid understanding of the data from the main triggers (e.g., trigger on bunch crossings at random to collect an unbiased data sample).

As for the LVL1 trigger, the HLT has a trigger menu that describes which events should be selected. This is illustrated in Table 2 for the example of CMS, assuming a luminosity for early running of $\mathcal{L} \sim 10^{33} \text{ cm}^{-2} \text{ s}^{-1}$. The total rate of $\sim 100 \text{ Hz}$ contains a large fraction of events that are useful for physics analysis. Lower thresholds would be desirable, but the physics coverage has to be balanced against considerations of the offline computing cost. Note that there are large uncertainties on the rate calculations.

Table 2: Estimated high-level trigger rates for $\mathcal{L} \sim 2 \times 10^{33} \text{ cm}^{-2} \text{ s}^{-1}$ (CMS numbers from Ref. [21])

Trigger configuration	Rate
One or more electrons with $p_T > 29 \text{ GeV}$, or two or more electrons with $p_T > 17 \text{ GeV}$	$\sim 34 \text{ Hz}$
One or more photons with $p_T > 80 \text{ GeV}$, or two or more photons with $p_T > 40, 25 \text{ GeV}$	$\sim 9 \text{ Hz}$
One or more muons with $p_T > 19 \text{ GeV}$, or two or more muons with $p_T > 7 \text{ GeV}$	$\sim 29 \text{ Hz}$
One or more taus with $p_T > 86 \text{ GeV}$, or two or more taus with $p_T > 59 \text{ GeV}$	$\sim 4 \text{ Hz}$
One or more jets with $p_T > 180 \text{ GeV}$ <i>and</i> missing- $E_T > 123 \text{ GeV}$	$\sim 5 \text{ Hz}$
One or more jets with $p_T > 657 \text{ GeV}$, or three or more jets with $p_T > 247 \text{ GeV}$, or four or more jets with $p_T > 113 \text{ GeV}$	$\sim 9 \text{ Hz}$
Others (electron and jet, b-jets, etc.)	$\sim 7 \text{ Hz}$

⁷Some triggers may be ‘pre-scaled’ — this means that only every N^{th} event satisfying the relevant criteria is recorded, where N is a parameter called the pre-scale factor; this is useful for collecting samples of high-rate triggers without swamping the T/DAQ system.

A major challenge lies in the HLT/DAQ software. The event-selection algorithms for the HLT can be subdivided, at least logically, into LVL2 and LVL3 trigger stages. These might be performed by two separate processor systems (e.g., ATLAS), or in two distinct processing steps within the same processor system (e.g., CMS). The algorithms have to be supported by a software framework that manages the flow of data, supervising an event from when it arrives at the HLT/DAQ system until it is either rejected, or accepted and recorded on permanent storage. This includes software for efficient transfer of data to the algorithms. In addition to the above, there is a large amount of associated online software (run control, databases, book-keeping, etc.).

11 LVL1 trigger design for the LHC

A number of design goals must be kept in mind for the LVL1 triggers at the LHC. It is essential to achieve a very large reduction in the physics rate, otherwise the HLT/DAQ system will be swamped and the dead-time will become unacceptable. In practice, the interaction rate, $\mathcal{O}(10^9)$ Hz, must be reduced to less than 100 kHz in ATLAS and CMS. Complex algorithms are needed to reject the background while keeping the signal events.

Another important constraint is to achieve a short latency — information from all detector elements ($\mathcal{O}(10^7\text{--}10^8)$ channels!) has to be held on the detector pending the LVL1 decision. The pipeline memories that do this are typically implemented in ASICs (application-specific integrated circuits), and memory size contributes to the cost. Typical LVL1 latency values are a few microseconds (e.g., less than 2.5 μs in ATLAS and less than 3.2 μs in CMS).

A third requirement is to have flexibility to react to changing conditions (e.g., a wide range of luminosities) and — it is hoped — to new physics! The algorithms must be programmable, at least at the level of parameters (thresholds, etc.).

11.1 Case study — ATLAS e/γ trigger

The ATLAS e/γ trigger algorithm can be used to illustrate the techniques used in LVL1 trigger systems at LHC. It is based on 4×4 ‘overlapping, sliding windows’ of trigger towers as illustrated in Fig. 19. Each trigger tower has a lateral extent of 0.1×0.1 in η, ϕ space, where η is pseudorapidity and ϕ is azimuth. There are about 3500 such towers in each of the EM and hadronic calorimeters. Note that each tower participates in calculations for 16 windows. The algorithm requires a local maximum in the EM calorimeter to define the η – ϕ position of the cluster and to avoid double counting of extended clusters (so-called ‘declustering’). It can also require that the cluster be isolated, i.e., little energy surrounding the cluster in the EM calorimeter or the hadronic calorimeter.

The implementation of the ATLAS LVL1 calorimeter trigger [25] is sketched in Fig. 20. Analog electronics on the detector sums signals from individual calorimeter cells to form trigger-tower signals. After transmission to the ‘pre-processor’ (PPr), which is located in an underground room close to the detector and shielded against radiation, the tower signals are received and digitized; then the digital data are processed to obtain estimates of E_T per trigger tower for each BC. At this point in the processing chain (i.e., at the output of the PPr), there is an ‘ η – ϕ matrix’ of the E_T per tower in each of the EM and hadronic calorimeters that gets updated every 25 ns.

The tower data from the PPr are transmitted to the cluster processor (CP). Note that the CP is implemented with very dense electronics so that there are only four crates in total. This minimizes the number of towers that need to be transmitted (‘fanned out’) to more than one crate. Fan out is required for towers that contribute to windows for which the algorithmic processing is implemented in more than one crate. Also, within each CP crate, trigger-tower data need to be fanned out between electronic modules, and then between processing elements within each module. Considerations of connectivity and data-movement drive the design.

In parallel with the CP, a jet/energy processor (JEP) searches for jet candidates and calculates

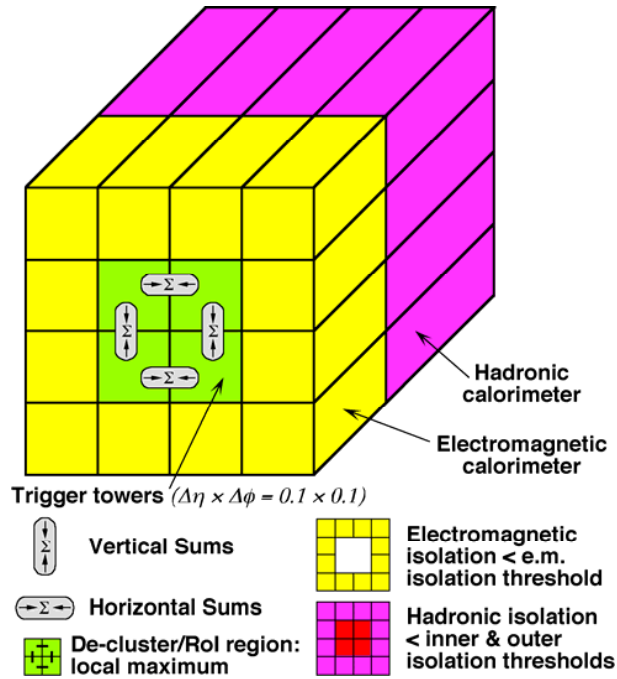


Fig. 19: ATLAS e/γ trigger algorithm

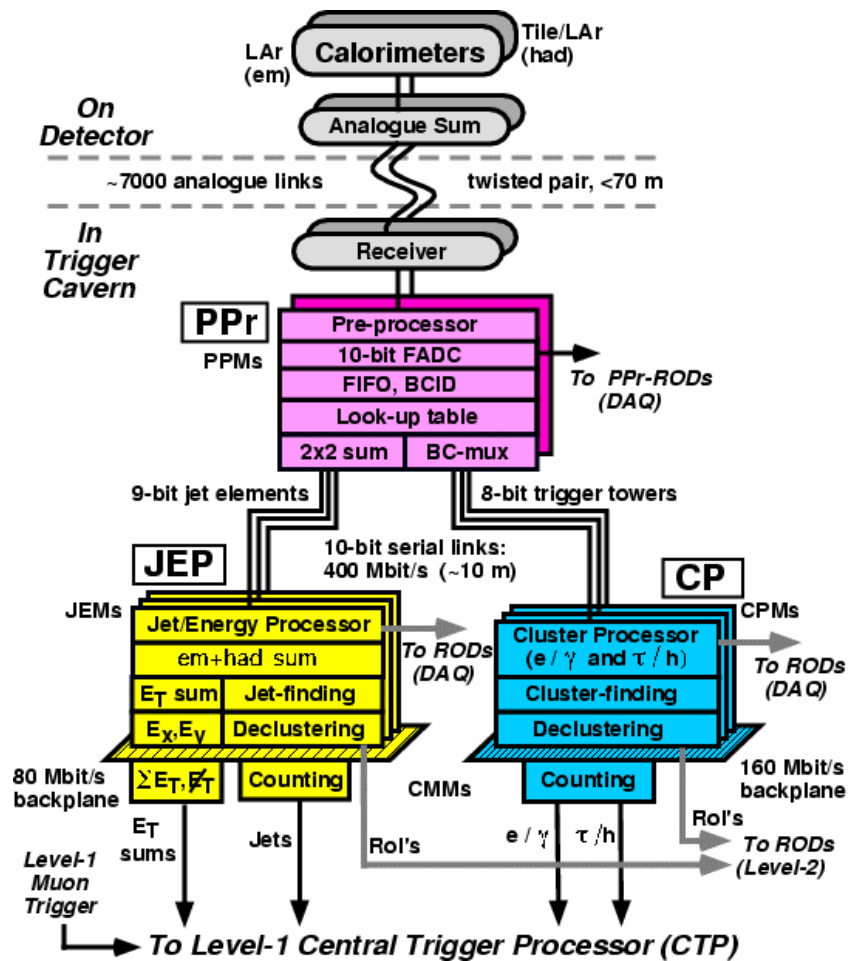


Fig. 20: Overview of the ATLAS LVL1 calorimeter trigger

missing- E_T and scalar- E_T sums. This is not described further here.

A very important consideration in designing the LVL1 trigger is the need to identify uniquely the BC that produced the interaction of interest. This is not trivial, especially given that the calorimeter signals extend over many BCs. In order to assign observed energy deposits to a given BC, information has to be combined from a sequence of measurements. Figure 21 illustrates how this is done within the PPr (the logic is repeated ~ 7000 times so that this is done in parallel for all towers). The raw data for a given tower move along a pipeline that is clocked by the 40 MHz BC signal. The multipliers together with the adder tree implement a finite-impulse-response filter whose output is passed to a peak finder (a peak indicates that the energy was deposited in the BC currently being examined) and to a look-up table that converts the peak amplitude to an E_T value. Special care is taken to avoid BC misidentification for very large pulses that may get distorted in the analog electronics, since such signals could correspond to the most interesting events. The functionality shown in Fig. 21 is implemented in ASICs (four channels per ASIC).

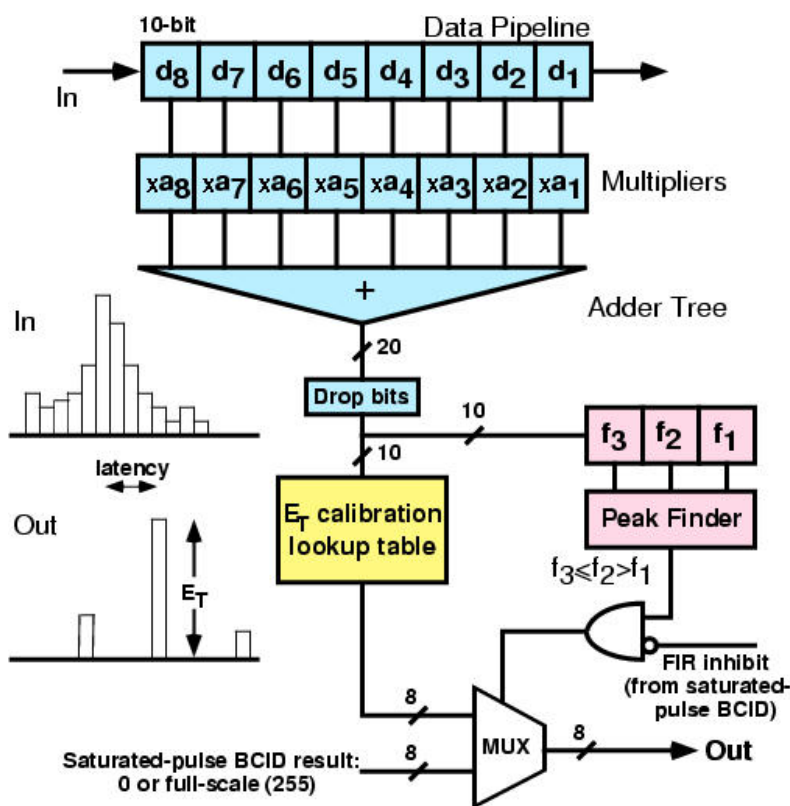


Fig. 21: Bunch-crossing identification

The transmission of the data (i.e., the E_T matrices) from the PPr to the CP is performed using a total of 5000 digital links each operating at 400 Mbits/s (each link carries data from two towers using a technique called BC multiplexing [25]). Where fan out is required, the corresponding links are duplicated with the data being sent to two different CP crates. Within each CP crate, data are shared between neighbouring modules over a very high density crate back-plane (~ 800 pins per slot in a 9U crate; data rate of 160 Mbits/s per signal pin using point-to-point connections). On each of the modules, data are passed to eight large field-programmable gate arrays (FPGAs) that perform the algorithmic processing, fanning out signals to more than one FPGA where required.

As an exercise, it is suggested that students make an order-of-magnitude estimate of the total bandwidth between the PPr and the CP, considering what this corresponds to in terms of an equivalent

number of simultaneous telephone calls⁸.

The e/γ (together with the τ/h) algorithms are implemented using FPGAs. This has only become feasible thanks to recent advances in FPGA technology since very large and very fast devices are needed. Each FPGA handles an area of 4×2 windows, requiring data from 7×5 towers in each of the EM and hadronic calorimeters. The algorithm is described in a programming language (e.g., VHDL) that can be converted into the FPGA configuration file. This gives flexibility to adapt algorithms in the light of experience — the FPGAs can be reconfigured *in situ*. Note that parameters of the algorithms can be changed easily and quickly, e.g., as the luminosity falls during the course of a coast of the beams in the LHC machine, since they are held in registers inside the FPGAs that can be modified at run time (i.e., there is no need to change the ‘program’ in the FPGA).

12 High-level trigger algorithms

There was not time in the lectures for a detailed discussion of the algorithms that are used in the HLT. However, it is useful to consider the case of the electron selection that follows after the first-level trigger. The LVL1 e/γ trigger is already very selective, so it is necessary to use complex algorithms and full-granularity, full-precision detector data in the HLT.

A calorimeter selection is made applying a sharper E_T cut (better resolution than at LVL1) and shower-shape variables that distinguish between the electromagnetic showers of an electron or photon on one hand, and activity from jets on the other hand. The shower-shape variables use both lateral and depth profile information. Then, for electrons, a requirement is made of an associated track in the inner detector, matching the calorimeter cluster in space, and with consistent momentum and energy measurements from the inner detector and calorimeter respectively.

Much work is going on to develop the algorithms and tune their many parameters to optimize their signal efficiency and background rejection. So far this has been done with simulated data, but further optimization will be required once samples of electrons are available from offline reconstruction of real data. It is worth noting that the efficiency value depends on the signal definition as shown in Fig. 22, an example of a study taken from Ref. [26]. Here the trigger efficiency is shown, as a function of electron transverse energy, relative to three different offline selections. With a loose offline selection, the trigger is comparatively inefficient, whereas it performs much better relative to the tighter offline cuts. This is related to the optimization of the trigger both for signal efficiency (where loose cuts are preferable) and for background rejection (where tighter cuts are required).

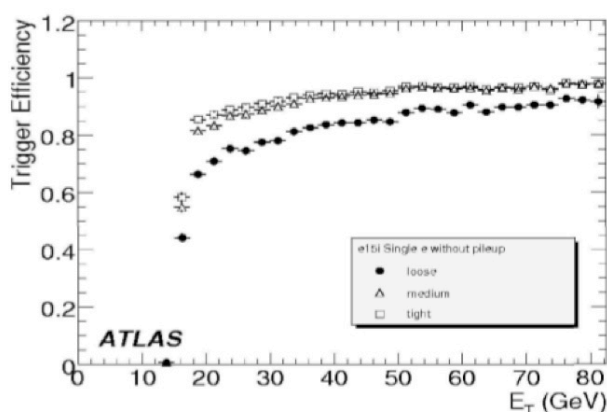


Fig. 22: Trigger efficiency versus electron E_T for three different offline selections of the reference sample

⁸One may assume an order-of-magnitude data rate for voice calls of 10 kbits/s — for example, the GSM mobile-phone standard uses a 9600 bit/s digital link to transmit the encoded voice signal.

13 Commissioning of the T/DAQ systems at LHC

Much more detail on the general commissioning of the LHC experiments can be found in the lectures of Andreas Hoecker at this School [27]. Here an attempt is made to describe how commissioning of the T/DAQ systems started in September 2008.

On 10 September 2008 the first beams passed around the LHC in both the clockwise and anti-clockwise directions, but with only one beam at a time (so there was no possibility of observing proton-proton collisions). The energy of the protons was 450 GeV which is the injection energy prior to acceleration; acceleration to higher energies was not attempted.

As a first step, the beams were brought around the machine and stopped on collimators such as those upstream of the ATLAS experiment. Given the huge number of protons per bunch, as well as the sizeable beam energy, extremely large numbers of secondary particles were produced, including muons that traversed the experiment depositing energy in all of the detector systems.

Next, the collimators were removed and the beams were allowed to circulate around the machine for a few turns and, after some tuning, for a few tens of turns. Subsequently, the beams were captured by the radio-frequency system of the LHC and circulated for periods of tens of minutes.

The first day of LHC operations was very exciting for all the people working on the experiments. There was a very large amount of media interest, with television broadcasts from various control rooms around the CERN site. It was a particularly challenging time for those working on the T/DAQ systems who were anxious to see if the first beam-related events would be identified and recorded successfully. Much to the relief of the author, the online event display of ATLAS soon showed a spectacular beam-splash event produced when the beam particles hit the collimator upstream of the experiment. The first ATLAS event is shown in Fig. 23; similar events were seen by the other experiments.

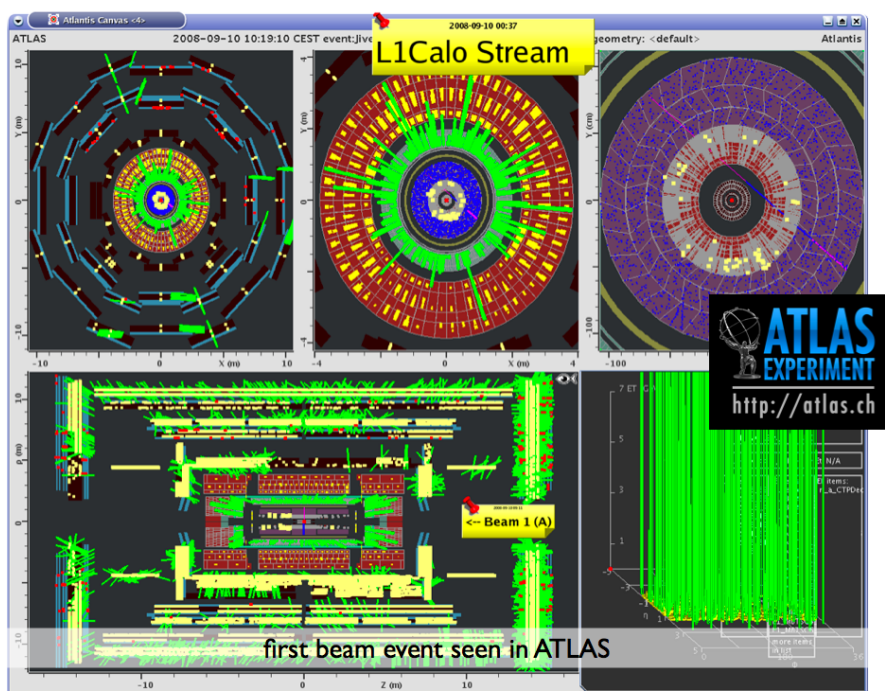


Fig. 23: The first beam-splash event in ATLAS

Analysis of the beam-splash events provided much useful information for commissioning the detectors and also the trigger. For example, the relative timing of different detector elements could be measured allowing the adjustment of programmable delays to the correct settings. The very large amount

of activity in the events had the advantage that signals were seen in an unusually large fraction of the detector channels.

An example of a very early study done with beam-splash events is shown in Fig. 24 which plots E_T versus η and ϕ for the ATLAS LVL1 calorimeter trigger readout. The E_T values are colour coded; η is along the x -axis and ϕ is along the y -axis. The eight-fold ϕ structure of the ATLAS magnets can be seen, as well as the effects of the tunnel floor and heavy mechanical support structures that reduced the flux of particles reaching the calorimeters in the bottom part of the detector ($\phi \approx 270$ degrees). The difference in absolute scale between the left-hand and right-hand sides of the plot is attributed to the fact that timing of the left-hand side was actually one bunch-crossing away from ideal when the data were collected; the timing calibration was subsequently adjusted as a result of these observations.

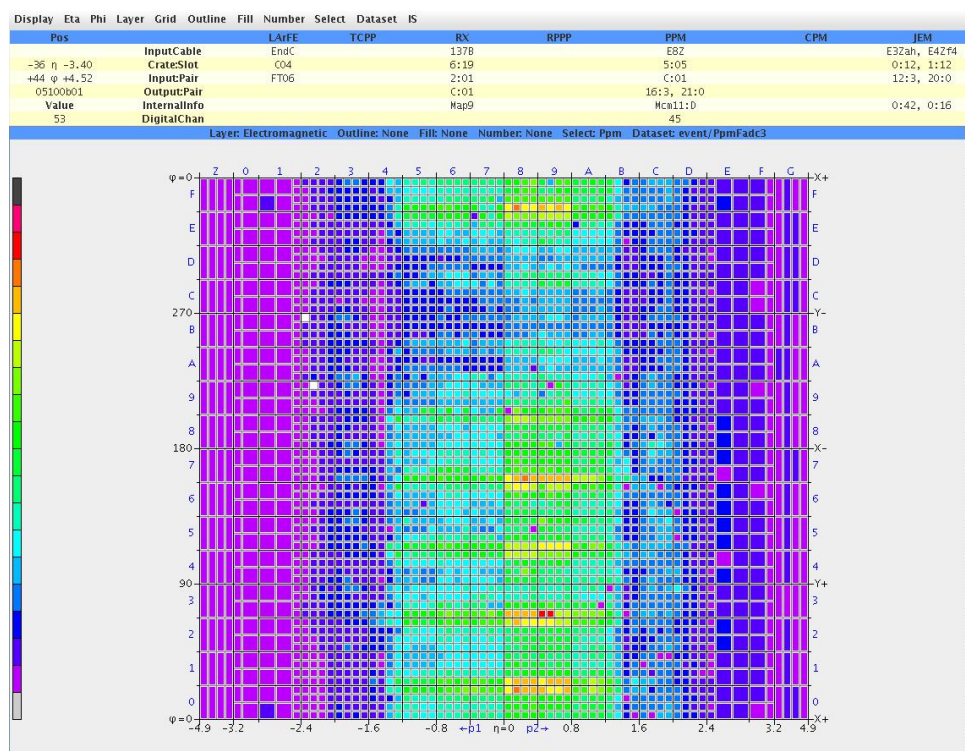


Fig. 24: LVL1 calorimeter trigger energy grid for a beam-splash event

At least in ATLAS, the first beam-splash events were recorded using triggers that had already been tested, with a free-running 40 MHz clock, for cosmic-ray events. This approach was appropriate because of the importance of recording the first beam-related activity in the detector before the local beam instrumentation had been calibrated. However, it was crucial to move on as rapidly as possible to establish a precise and stable time reference.

Once beam-related activity had been seen in all of the LHC experiments, stopping the beam on the corresponding collimators, all of the collimators were removed and the beam was allowed to circulate. The first circulating beams passed around the LHC for only a short period of time, corresponding to a few turns initially, rising to a few tens of turns. For the 27 km LHC circumference, the orbit period is about 89 μ s.

Upstream of the LHC detectors (and upstream of the collimators) are passive beam pick-ups that provide electrical signals induced by the passage of the proton beams. The photograph in the left-hand side of Fig. 25 shows the beam pick-up for one of the beams in an LHC experiment. Three of the four cables that carry the signals can be seen. The analog signals from electrodes above, below, to the left and to the right of the beam are combined (analog sum). The resulting signal is fed to an oscilloscope

directly and also via a discriminator (an electronic device that provides a logical output signal when the analog input signal exceeds a preset threshold, see Section 2).

On the right-hand side of Fig. 25 can be seen a plot, from CMS, of the relative timing of different signals. The upper three traces are ‘orbit’ signals provided by the LHC machine, whereas the bottom trace is the discriminated beam pick-up signal. As can be seen, the pick-up signal is present for only four turns and then disappears. The reason for this is that after a few turns the protons de-bunched and the analog signal from the pick-ups became too small to fire the discriminator. Similar instrumentation and timing calibration studies were used in all of the LHC experiments.



Fig. 25: Photograph of beam pick-up instrumentation (left) and display of timing signals recorded on a digital oscilloscope (right). The upper three traces are ‘orbit’ signals from the LHC machine, whereas the bottom one is the (inverted) discriminated signal from the beam pick-up.

A key feature of the beam pick-ups is that they provide a stable time reference with respect to which other signals can be aligned. The time of arrival of the beam pick-up signal, relative to the moment when the beam passes through the centre of the LHC detector, depends only on the proton time of flight from the beam pick-up position to the centre of the detector, propagation delays of the signal along the electrical cables, and the response time of the electronic circuits (which is very short).

Thanks to thorough preparations, the beam pick-up signals and their timing relative to the trigger could be measured as soon as beam was injected. Programmable delays could then be adjusted to align in time inputs to the trigger from the beam pick-ups and from other sources. For example, in ATLAS, the beam pick-up inputs were delayed so that they would have the same timing as other inputs that had already been adjusted using cosmic-rays.

Once the timing of the beam pick-up inputs to the trigger had been adjusted so as to initiate the detector readout for the appropriate bunch crossing (BC), i.e., to read out a time-frame that would contain the detector signals produced by beam-related activity, they could be used to provide the trigger for subsequent running.

It is worth noting that the steps described above to set up the timing of the trigger were completed

within just a few hours on the morning of 10 September 2008. From then onwards the beam pick-ups represented a stable time reference with respect to which other elements in the trigger and in the detector readout systems could be adjusted.

As already indicated, all of the beam operations in September 2008 were with just a single beam in the LHC. Operations were performed with beams circulating in both the clockwise and anti-clockwise directions. Beam activity in the detectors was produced by beam splash (beam stopped on collimators upstream of the detectors producing a massive number of secondary particles) or by beam-halo particles (produced when protons lost from the beam upstream of the detectors produced one or more high-momentum muons that traversed the detectors). In both cases one has to take into account the time of flight of the particles that reach one end of the detector before the other end. In contrast, beam–beam interactions have symmetric timing for the two ends of the detector.

The work on timing calibration performed over the days following the LHC start up can be illustrated by the case of ATLAS. Already on 10 September both sets of beam pick-ups had been commissioned (with beams circulating in the clockwise and anti-clockwise directions) giving a fixed time reference with respect to which the rest of the trigger, and indeed the rest of the experiment, could be aligned.

The situation on 10 September is summarized in the left-hand plot of Fig. 26. The beam pick-up signal, labelled ‘BPTX’ in the figure, is the reference. The relative time of arrival of other inputs to the trigger is shown in units of BC number (i.e. one unit corresponds to 25 ns which is the nominal bunch-crossing interval at LHC). Although there is a peak at the nominal timing (bunch-number zero) in the distributions based on different trigger inputs — the Minimum-Bias Trigger Scintillators (MBTS), the Thin-Gap Chamber (TGC) forward muon detectors, and the Tau5, J5 and EM3 items from the calorimeter trigger — the distribution is broad.

Prompt analysis and interpretation of the data allowed the timing to be understood and calibration corrections to be applied. Issues addressed included programming delay circuits to correct for time of flight of the particles according to the direction of the circulating beam and tuning the relative timing of triggers from different parts of the detector or from different detector channels.

The situation two days later on 12 September is summarized in the right-hand plot of Fig. 26. It is important to note that the scale is logarithmic — the vast majority of the triggers are aligned correctly in the nominal bunch crossing. Although shown in the plot, the input from the Resistive Plate Chambers (RPC) barrel muon detectors, which see very little beam-halo activity in single-beam operation, had not been timed-in.

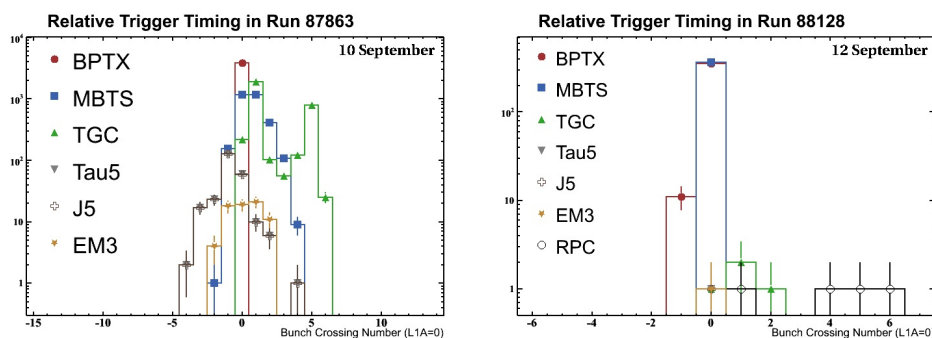


Fig. 26: Progress on timing-in ATLAS between 10 and 12 September 2008

As can be seen from the above, very significant progress was made on setting up the timing of the experiments within the first few days of single-beam operations at LHC. The experimental teams were eagerly awaiting further beam time and the first collisions that would have allowed them to continue the work. However, unfortunately, on 19 September there was a serious accident with the LHC machine that

required a prolonged shutdown for repairs and improvements. Nevertheless, when the LHC restarts one will be able to build on the work that was already done (complemented by many further studies that were done using cosmic rays during the machine shutdown).

A huge amount of work has been done using the beam-related data that were recorded in September 2008, as discussed in much more detail in the lectures of Andreas Hoecker at this School [27]. A very important feature of these data is that activity is seen in the same event in several detector subsystems which allows one to check the relative timing and spatial alignment. Indeed the fact that the same event is seen in the different subdetectors is reassuring — some previous experiments had teething problems where the readout of some of the subdetectors became desynchronized! A nice example of a beam-halo event recorded in CMS is shown in Fig. 27. Activity can be seen in the Cathode-Strip Chamber (CSC) muon detectors at both ends of the experiment and also in the hadronic calorimeter.

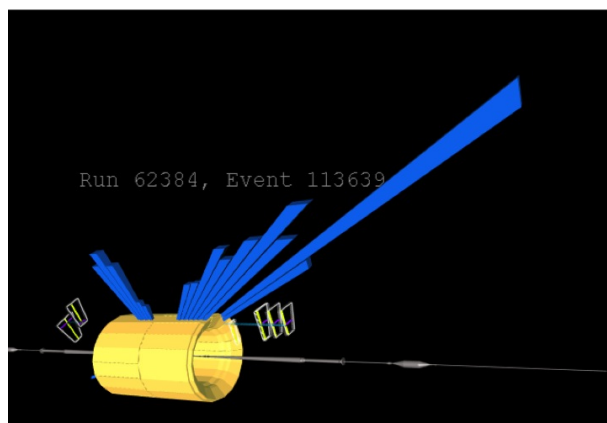


Fig. 27: A beam-halo event in CMS

The detectors and triggers that were used in September 2008 were sensitive to cosmic-ray muons as well as to beam-halo particles when a requirement of a signal from the beam pick-ups was not made. The presence of beam-halo and cosmic-ray signals in the data is illustrated in Fig. 28 which shows the angular distribution of muons reconstructed in CMS. The shape of the cosmic-ray distribution, which has a broad peak centred around 0.3–0.4 radians, is known from data collected without beam. The peak at low angles matches well with the distribution for simulated beam-halo particles.

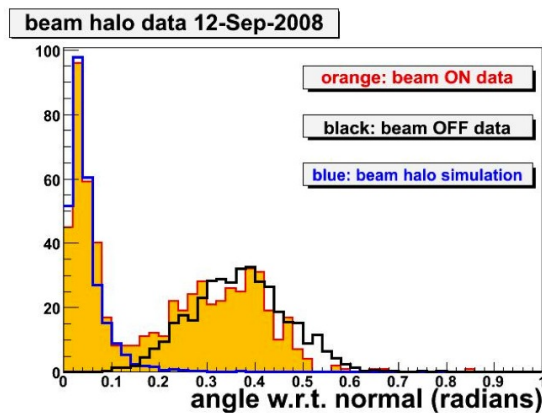


Fig. 28: Angular distribution of muons in CMS recorded with and without circulating beam. Also shown is the distribution for simulated beam-halo events.

Before concluding, the author would like to show another example of a study with single-beam data. Using a timing set-up in the end-cap muon trigger that would be appropriate for colliding-beam operations, in which the muons emerge from the centre of the apparatus, the distribution shown in the right-hand part of Fig. 29 was obtained. The two peaks separated by four bunch crossings, i.e., 4×25 ns, correspond to triggers seen in the two ends of the detector system. This is consistent within the resolution with the time of flight of the beam-halo particles that may trigger the experiment on the upstream or downstream sides of the detector. As indicated in the left-hand part of the figure, this is reminiscent of the very simple example that was introduced early on in the lectures, see Fig. 1.

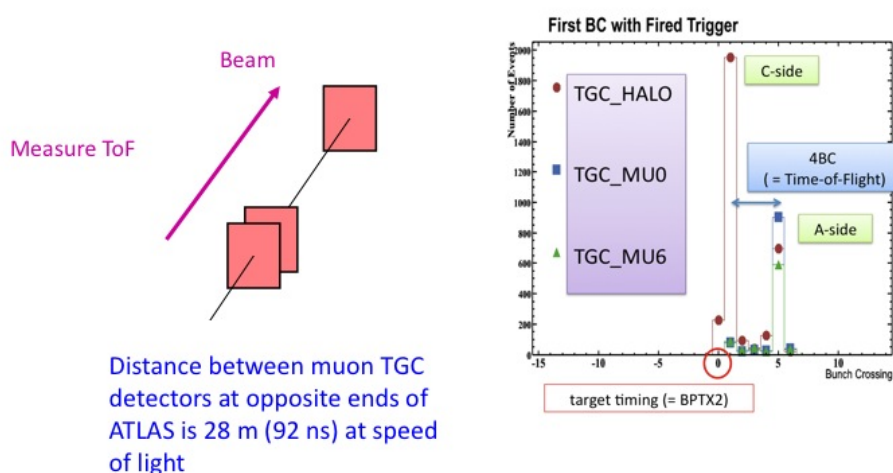


Fig. 29: Time of flight of beam-halo muons in ATLAS (one BC is 25 ns)

14 Concluding remarks

It is hoped that these lectures have succeeded in giving some insight into the challenges of building T/DAQ systems for HEP experiments. These include challenges connected with the physics (inventing algorithms that are fast, efficient for the physics of interest, and that give a large reduction in rate), and challenges in electronics and computing. It is also hoped that the lectures have demonstrated how the subject has evolved to meet the increasing demands, e.g., of LHC compared to LEP, by using new ideas based on new technologies.

Acknowledgements

The author would like to thank the local organizing committee for their wonderful hospitality during his stay in Colombia. In particular, he would like to thank Marta Losada and Enrico Nardi who, together, created such a wonderful atmosphere between all the participants, staff and students alike.

The author would like to thank the following people for their help and advice in preparing the lectures and the present notes: Bob Blair, Helfried Burckhart, Vincenzo Canale, Philippe Charpentier, Eric Eisenhandler, Markus Elsing, Philippe Farthouat, John Harvey, Andreas Hoecker, Jim Linnerman, Claudio Luci, Jordan Nash, Thilo Pauly, and Wesley Smith.

References

- [1] L. Evans and P. Bryant (eds.), LHC machine, *JINST* **3** S08001 (2008).
- [2] R.W. Assmann, M. Lamont, and S. Myers, A brief history of the LEP collider, *Nucl. Phys. B, Proc. Suppl.* **109** (2002) 17–31, <http://cdsweb.cern.ch/record/549223>.
- [3] <http://en.wikipedia.org/wiki/NIM>
- [4] http://en.wikipedia.org/wiki/Computer_Automated_Measurement_and_Control
- [5] J. Schukraft, Heavy-ion physics at the LHC, in Proceedings of the 2003 CERN–CLAF School of High-Energy Physics, San Miguel Regla, Mexico, CERN-2006-001 (2006).
ALICE Collaboration, Trigger, Data Acquisition, High Level Trigger, Control System Technical Design Report, CERN-LHCC-2003-062 (2003).
The ALICE Collaboration, K. Aamodt et al., The ALICE experiment at the CERN LHC, *JINST* **3** S08002 (2008) and references therein.
- [6] J. Nash, these proceedings.
- [7] C. Amsler et al. (Particle Data Group), *Phys. Lett. B* **667** (2008) 1 also available online from <http://pdg.lbl.gov/>.
- [8] W. von Rueden, The ALEPH data acquisition system, *IEEE Trans. Nucl. Sci.* **36** (1989) 1444–1448.
J. F. Renardy et al., Partitions and trigger supervision in ALEPH, *IEEE Trans. Nucl. Sci.* **36** (1989) 1464–1468.
A. Belk et al., DAQ software architecture for ALEPH, a large HEP experiment, *IEEE Trans. Nucl. Sci.* **36** (1989) 1534–1539.
P. Mato et al., The new slow control system for the ALEPH experiment at LEP, *Nucl. Instrum. Methods A* **352** (1994) 247–249.
- [9] A. Augustinus et al., The DELPHI trigger system at LEP2 energies, *Nucl. Instrum. Methods A* **515** (2003) 782–799.
DELPHI Collaboration, Internal Notes DELPHI 1999-007 DAS 188 and DELPHI 2000-154 DAS 190 (unpublished).
- [10] B. Adeva et al., The construction of the L3 experiment, *Nucl. Instrum. Methods A* **289** (1990) 35–102.
T. Angelov et al., Performances of the central L3 data acquisition system, *Nucl. Instrum. Methods A* **306** (1991) 536–539.
C. Dionisi et al., The third level trigger system of the L3 experiment at LEP, *Nucl. Instrum. Methods A* **336** (1993) 78–90 and references therein.
- [11] J.T.M. Baines et al., The data acquisition system of the OPAL detector at LEP, *Nucl. Instrum. Methods A* **325** (1993) 271–293.
- [12] <http://en.wikipedia.org/wiki/VMEbus>
- [13] H1 Collaboration, The H1 detector, *Nucl. Instrum. Methods A* **386** (1997) 310.
- [14] R. Carlin et al., The trigger of ZEUS, a flexible system for a high bunch crossing rate collider, *Nucl. Instrum. Methods A* **379** (1996) 542–544.
R. Carlin et al., Experience with the ZEUS trigger system, *Nucl. Phys. B, Proc. Suppl.* **44** (1995) 430–434.
W.H. Smith et al., The ZEUS trigger system, CERN-92-07, pp. 222–225.
- [15] CDF IIb Collaboration, The CDF IIb Detector: Technical Design Report, FERMILAB-TM-2198 (2003).
- [16] D0 Collaboration, RunIIb Upgrade Technical Design Report, FERMILAB-PUB-02-327-E (2002).
- [17] R. Arcidiacono et al., The trigger supervisor of the NA48 experiment at CERN SPS, *Nucl. Instrum. Methods A* **443** (2000) 20–26 and references therein.
- [18] T. Fuljahn et al., Concept of the first level trigger for HERA-B, *IEEE Trans. Nucl. Sci.* **45** (1998)

1782–1786.

M. Dam et al., Higher level trigger systems for the HERA-B experiment, *IEEE Trans. Nucl. Sci.* **45** (1998) 1787–1792.

- [19] ATLAS Collaboration, First-Level Trigger Technical Design Report, CERN-LHCC-98-14 (1998).
ATLAS Collaboration, High-Level Triggers, Data Acquisition and Controls Technical Design Report, CERN-LHCC-2003-022 (2003).
- [20] The ATLAS Collaboration, G. Aad et al., The ATLAS experiment at the CERN Large Hadron Collider, *JINST* **3** S08003 (2008) and references therein.
- [21] CMS Collaboration, The Level-1 Trigger Technical Design Report, CERN-LHCC-2000-038 (2000).
CMS Collaboration, Data Acquisition and High-Level Trigger Technical Design Report, CERN-LHCC-2002-26 (2002).
- [22] The CMS Collaboration, S. Chatrchyan et al., The CMS experiment at the CERN LHC, *JINST* **3** S08004 (2008) and references therein.
- [23] See, for example, summary talks in Proc. Computing in High Energy and Nuclear Physics, CHEP 2003, <http://www.slac.stanford.edu/econf/C0303241/proceedings.html>
- [24] LHCb Collaboration, Online System Technical Design Report, CERN-LHCC-2001-040 (2001).
LHCb Collaboration, Trigger System Technical Design Report, CERN-LHCC-2003-031 (2003).
The LHCb Collaboration, A. Augusto Alves Jr et al., The LHCb detector at the LHC, *JINST* **3** S08005 (2008) and references therein.
- [25] R. Achenbach et al., The ATLAS level-1 calorimeter trigger, *JINST* **3** P03001 (2008).
- [26] G. Navara et al., Electron trigger performance of the ATLAS detector, presented at *Signaling the Arrival of the LHC Era*, Trieste, Italy, 8–13 December 2008.
- [27] A. Hoecker, these proceedings.